(p)ppGpp modifies RNAP function to confer β-lactam resistance in a peptidoglycan-independent manner

Henri Voedts, Constantin Anoyatis-Pelé, Olivier Langella, Filippo Rusconi, Jean-Emmanuel Hugonnet, Michel Arthur

(p)ppGpp modifies RNAP function to confer β-lactam resistance in a peptidoglycan-independent manner

Henri Voedts[1+], Constantin Anoyatis-Pelé[1+], Olivier Langella[2], Filippo Rusconi[1,2], Jean-Emmanuel Hugonnet[1#*], and Michel Arthur[1#*]

[1] Centre de Recherche des Cordeliers, Sorbonne Université, INSERM, Université Paris Cité, F-75006 Paris, France.

[2] GQE-Le Moulon/PA, Université Paris-Saclay, INRAE, CNRS, AgroParisTech, IDEEV ; 12, route 128 ; F-91272 Gif-sur-Yvette, France.

[+] Equal contributions

[#] Equal contributions

* Corresponding authors: michel.arthur@crc.jussieu.fr; jean-emmanuel.hugonnet@crc.jussieu.fr

Little is known on the adaptation of the cell wall peptidoglycan metabolism to nutrient deprivation. We hypothesized that (p)ppGpp might be involved in this process since elevated levels of this alarmone confer resistance to the narrow-spectrum β-lactam mecillinam. In addition, (p)ppGpp is essential for broad-spectrum β-lactam resistance mediated by redirecting the flux of peptidoglycan precursors toward the β-lactam-insensitive transpeptidase YcbB (LdtD). High-resolution mass spectrometry analyses of peptidoglycan structure unexpectedly revealed that these (p)ppGpp-dependent resistance mechanisms do not rely on any modification of peptidoglycan metabolism. Amino acid substitutions in the β or β' RNA polymerase (RNAP) subunits, alone or in combination with the CRISPR interference-mediated downregulation of three of seven ribosomal RNA operons, was sufficient for resistance, although β-lactams have no known impact on the RNAP or ribosomes. This implies that modifications of RNAP and ribosome functions are critical to prevent downstream effects of the inactivation of peptidoglycan transpeptidases by β-lactams.

The ubiquitous stringent response is triggered in response to diverse stresses, such as amino acid or phosphate starvation[1,2]. The stringent response relies on the production of the alarmones ppGpp (guanosine 5′-diphosphate 3′-diphosphate) and pppGpp (guanosine 5′-triphosphate 3′-diphosphate) [collectively referred to as (p)ppGpp]. In *Escherichia coli*, (p)ppGpp production involves two homologues of (p)ppGpp synthases, named RelA and SpoT. RelA is a monofunctional enzyme that possesses only (p)ppGpp synthase activity while SpoT is a bifunctional enzyme with both (p)ppGpp synthetic and hydrolytic activities. The (p)ppGpp alarmone binds to and directly activates or inhibits several enzymes involved in multiple metabolic pathways (Fig. 1)[3]. In *E. coli*, the alarmone also modulates the expression of *ca*. 1200 genes by binding to the RNA polymerase (RNAP) and altering its promoter selectivity and the stability of the initiation complex[2,4].

Peptidoglycan is an essential macromolecule that surrounds the bacterial cell providing resistance to the turgor pressure of the cytoplasm[5]. The disaccharide-pentapeptide subunit of peptidoglycan is polymerized to form glycan strands cross-linked by short peptides. D,D-transpeptidases belonging to the penicillin-binding protein (PBP) family form 4→3 cross-links connecting the fourth residue (D-Ala^4) of an acyl donor stem to the third residue (DAP^3) of an acyl acceptor stem (Extended Data Fig. 1a). The unrelated L,D-transpeptidases (LDTs) catalyze the formation of 3→3 cross-links connecting two DAP^3 residues (Extended Data Fig. 1b). PBPs and LDTs show distinct inhibition profiles since PBPs are potentially inhibited by all classes of β-lactams (including penams, cephems, and carbapenems), whereas LDTs are effectively inhibited only by carbapenems[6]. Bypass of PBPs by LDTs, which leads to high-level resistance to β-lactams of the penam (such as ampicillin) and cephem (ceftriaxone) classes, was previously reported in recombinant *E. coli* strains that overproduce the YcbB L,D-transpeptidase (also known as LdtD) and the (p)ppGpp alarmone[7]. (p)ppGpp production that activates YcbB-mediated β-lactam resistance was triggered either by (i) mutations that impair the activity of aminoacyl-tRNA synthetases and mimic amino acid starvation, leading to the activation of the (p)ppGpp synthase activity of RelA or by (ii) expression of a truncated allele of *relA* that encodes the RelA' synthase mediating constitutive production of (p)ppGpp. In the absence of the YcbB L,D-transpeptidase, elevated (p)ppGpp on its own leads to high-level resistance to the narrow spectrum β-lactam mecillinam, which specifically inactivates PBP2, a peptidoglycan D,D-transpeptidase involved in cell elongation[8].

The role of (p)ppGpp in resistance to mecillinam and to broad-spectrum β-lactams mediated by YcbB implies a functional link between peptidoglycan synthesis and the stringent response. The nature of this link remains fully unknown. This is surprising since (p)ppGpp-mediated mecillinam-resistance was reported 30 years ago. Furthermore, mecillinam has been extensively used as a chemical probe for exploring both peptidoglycan polymerization and the mode of action of β-lactams. The pleiotropic effects of (p)ppGpp may account for this knowledge gap. Here, we investigate every aspect of (p)ppGpp-mediated regulation and narrow its role in β-lactam resistance down to specific alterations of RNAP and ribosomal functions. The structure of peptidoglycan was not modified in response to these alterations indicating that their contribution to β-lactam resistance did not rely on regulatory effects on genes involved in peptidoglycan metabolism. We discuss the impact of these controls in the light of recent models accounting for the cascade of events triggered by inactivation of peptidoglycan polymerases by β-lactams.

RESULTS

High levels of (p)ppGpp do not alter peptidoglycan structure. Our first objective was to determine whether (p)ppGpp directly affects peptidoglycan composition. In the absence of induction of the plasmid copy of the *ycbB* gene by IPTG, production of the (p)ppGpp synthase following induction of gene *relA'* did not lead to any modification of peptidoglycan structure (Fig. 2a, 2c, and 2d). In this condition, the proportion of peptidoglycan dimers containing 3→3 cross-links was low. In contrast, induction of *ycbB* alone resulted in an increase in the proportion of 3→3 cross-linked dimers and overall peptidoglycan cross-linking (Fig. 2b, 2c, and 2d). Additional induction of *relA'* did not result in further modifications of the peptidoglycan structure. These observations indicate that the alarmone does not modulate the activity of enzymes specifically involved in peptidoglycan polymerization. The formal possibility that production of (p)ppGpp might alter the expression of the chromosomal copy of *ycbB* was ruled out by repeating the peptidoglycan analysis in strains lacking the chromosomal copy of this gene (Extended Data Fig. 2).

Bypass of (p)ppGpp by mutational alteration of RNA polymerase. Our second objective was to determine whether the essential role of the (p)ppGpp alarmone in YcbB-mediated β-lactam

resistance depends upon modulation of RNA polymerase activity or upon direct binding to other enzymes. To address this question, we anticipated that mutations enabling expression of β-lactam resistance in a Δ*relA* Δ*spoT* background [(p)ppGpp^0] would map in the gene(s) encoding the alarmone target(s) responsible for resistance and thereby lead to their identification. YcbB-expressing mutants resistant to all β-lactams except carbapenems, the hallmark of bypass of PBPs by YcbB, were obtained at a frequency of *ca*. 2 x 10^{-8} in media containing the broad-spectrum β-lactam ampicillin. Genome sequencing of 5 mutants revealed 4 distinct single mutations leading to 4 distinct amino acid substitutions in the β or β' RNAP subunits (Fig. 3a). This observation indicates that the role of (p)ppGpp in YcbB-mediated β-lactam resistance depends upon modulation of RNAP activity and not upon direct binding of (p)ppGpp to other enzymes.

Our next objective was to extend our analysis to mutants selected on media containing mecillinam in the absence of induction of *ycbB*. Mutants selected on this medium (frequency of *ca.* 3 x 10^{-8}) were all (12 out of 12) additionally resistant to all other β-lactams except carbapenems upon induction of *ycbB* by IPTG and harbored 10 distinct mutations leading to 10 distinct substitutions in the β or β' RNAP subunits (Fig. 3a). Thus, dissociated resistance to mecillinam or to ampicillin (upon *ycbB* induction) was not observed indicating that (p)ppGpp has similar roles in mecillinam resistance and in YcbB-mediated broad-spectrum β-lactam resistance. For the sake of simplicity, we will hereafter refer to β-lactam resistance to designate mecillinam resistance in the absence of *ycbB* induction combined to resistance to cephems and penams upon induction of this gene.

RNAP is the target of rifampicin and substitutions leading to resistance to this drug are mostly clustered in narrow regions of the RNAP β subunit[9] that was shown here to also contain substitutions selected on media containing β-lactams (above, Fig. 3a and Extended Data Fig. 3a). Strikingly, pioneering work on (p)ppGpp-mediated mecillinam resistance revealed that rifampicin at sub-inhibitory concentrations abolishes resistance to mecillinam[8]. The synergy between the two drugs prompted us to determine whether selection for resistance to β-lactams or rifampicin results in dissociated or co-resistance to these drugs. The collection of 17 mutants selected on β-lactams was screened for expression of rifampicin resistance revealing co-resistance in 8 of 17 mutants (Fig. 3a). Conversely, mutants selected on rifampicin (frequency of *ca.* 9 x 10^{-7}) harbored mutations in the RNAP β subunit (10 out of 10; 5 distinct mutations; 5 distinct amino acid substitutions) and were resistant to rifampicin only (4 out of

10 mutants, 4 distinct amino acid substitutions) or co-resistant to β-lactams (6 out of 10; 1 distinct amino acid substitution). These results indicate that substitutions in the β or β' RNAP subunits result both in dissociate and co-resistance to β-lactams and rifampicin. Substitutions conferring co-resistance to β-lactams and rifampicin both mimic binding of (p)ppGpp to RNAP, thereby leading to β-lactam resistance, and prevent binding of rifampicin to RNAP. Although the modes of action of β-lactams and rifampicin differ, these results demonstrate the possible emergence of cross-resistance in clinical isolates, a so-far neglected aspect of these two widely used antibiotics. Of note, cross-resistance to rifampicin and the β-lactam cefuroxime in a mutant selected in laboratory conditions was reported to result from the $Ser^{487}Leu$ substitution in *Bacillus subtilis* RpoB, which is distinct from those reported in Fig. 3a for *E. coli*[10].

RNAP (p)ppGpp binding site 2 is critical for β-lactam resistance. Since RNAP harbors two (p)ppGpp binding sites, our next objective was to determine whether β-lactam resistance is specifically controlled by binding of the alarmone to one of these sites. These sites are located at the interfaces defined by the β' subunit and either the ω subunit (site 1) or transcription factor DksA (site 2)[11,12]. Since the alarmone does not bind to site 1 or 2 in the absence of the ω subunit or DksA, respectively, we independently deleted the corresponding genes to disrupt either (p)ppGpp binding site. Deletion of *dksA* but not that of *rpoZ* abolished expression of β-lactam resistance, indicating that resistance requires binding of the alarmone to site 2 but not to site 1 (Extended Data Fig. 4). In agreement, the RNAP substitutions enabling β-lactam resistance in the $(p)ppGpp^0$ background were closer to site 2 than to site 1 (Fig. 3b) and were clustered at positions in or very close to the path of DNA in the transcription complex, possibly causing a reduction in the stability of the RNAP-promoter open complex (Extended Data Fig. 3b)[9]. The overexpression of *dksA*, known to modulate transcription on its own[13,14], bypassed the requirement of (p)ppGpp for β-lactam resistance (see below). Together, these results suggest that β-lactam resistance requires a modulation of RNAP activity mediated by binding of the alarmone to site 2. This effect can be mimicked by modification of residues in the β and β' RNAP subunits or by overproduction of DksA.

A negative control of the growth rate is not sufficient for β-lactam resistance. Since the intracellular concentration of (p)ppGpp is one of the factors that affect growth rate[15], we

considered the possibility that β-lactam resistance might merely depend upon this global effect. To investigate this possibility, we determined the growth rate of 12 mutants representative of dissociate and co-resistance to β-lactams and rifampicin (Fig. 3a). Strikingly, all mutants, irrespective of their resistance phenotype, had an increased generation time compared to the parental strain. For instance, one mutant (harboring the $Gly^{449}Val$ substitution) was resistant to β-lactams but another (harboring the $Gln^{148}Leu$ substitution) was susceptible to β-lactams in spite of a similarly increased generation time (27 ± 1 min *vs.* 28 ± 2 min, respectively, instead of 24 ± 1 min for the parental strain) (see Extended Data Fig. 5 for the resistance phenotypes conveyed by the $Gly^{449}Val$ and $Gln^{148}Leu$ substitutions). In addition, supplementation of the growth medium with sub-inhibitory concentrations of chloramphenicol resulted in a dose-dependent increase in the generation time without enabling ceftriaxone resistance (Extended Data Fig. 6a and 6b). Furthermore, growth at 28 °C instead of 37 °C also resulted in an increase in the generation time and the absence of expression of β-lactam resistance (Extended Data Fig. 6c). These analyses revealed that a reduced growth rate was not, in itself, sufficient for β-lactam resistance. The role of (p)ppGpp in β-lactam resistance does not only depend upon a negative control of the growth rate, that might have, for example, compensated for ineffective peptidoglycan polymerization in the presence of the drugs.

Single-gene overexpression identified *dksA* as the only gene bypassing (p)ppGpp for β-lactam resistance. To identify (p)ppGpp-regulated genes specifically involved in β-lactam resistance, we first investigated unique genes by using the ASKA plasmid library, which enables IPTG-inducible overexpression of each individual gene of the *E. coli* genome[16]. Selection for a bypass of the (p)ppGpp requirement for β-lactam resistance revealed the same DksA-encoding plasmid in 40 out of 40 transformants. These results suggest that the essential role of (p)ppGpp in β-lactam resistance cannot be accounted for by the upregulation of a single gene. However, the impact of the upregulation of a combination of several genes cannot be assessed by this experimental approach.

(p)ppGpp does not mediate β-lactam resistance by modulating the activity of alternative sigma factors. Since the various effects of (p)ppGpp on gene transcription include the recruitment of alternative sigma factors by RNAP (Fig. 1)[17,18], we investigated the possibility

that the role of (p)ppGpp in β-lactam resistance could involve increased transcription of a set of genes controlled by a specific sigma factor[19–21]. Four of the six alternative sigma factors were directly evaluated by gene deletion as they are dispensable for growth in *E. coli*. Deletion of genes *rpoN*, *rpoS*, *rpoF*, or *fecI*, encoding the unessential sigma factors σ^N (σ^{54}), σ^S (σ^{38}), σ^F (σ^{28}), and σ^{FecI} (σ^{19}), respectively, did not abolish resistance to β-lactams (Extended Data Table 1). As a complementary approach, we designed an experiment to test the impact of overproduction of each one of the six alternative sigma factors on the expression of β-lactam resistance. The rationale for this experiment arises from the possibility that overproduction of these alternative factors could lead to effective competition with the vegetative sigma factor σ^D for binding to the RNAP core enzyme, thereby mimicking the (p)ppGpp-dependent increased affinity of RNAP for the alternative sigma factors. Overproduction of the essential (σ^H and σ^E) and unessential (σ^N, σ^S, σ^F, and σ^{FecI}) sigma factors was obtained by cloning the corresponding genes in the expression vector pHV7. Overproduction of the six alternative sigma factors did not bypass the requirement of (p)ppGpp for β-lactam resistance in any of the genetic backgrounds tested (Extended Data Table 1). Together, these results indicate that modulation of the transcription of specific genes by alternative sigma factors does not account for the essential role (p)ppGpp in β-lactam resistance.

Downregulation of ribosomal RNA operons mediates β-lactam resistance in combination with a specific alteration of the β RNAP subunit. Since binding of (p)ppGpp to the RNAP results in a decrease in the number of ribosomes per cell mediated by the downregulation of the operons encoding ribosomal RNA genes[13,22,23] (Fig. 1) our last objective was to determine whether a decrease in the transcription of ribosomal RNAs could contribute to β-lactam resistance. The CRISPR interference (CRISPRi) approach[24] was therefore used to downregulate the transcription of multiple *rrn* operons at once (Fig. 4a and Extended Data Fig. 7a for the rationale underlying the design of the RNA guides). To guide dCas9 on the *rrn* operons, we independently cloned in the pFR56 plasmid four different single-guide RNAs (sgRNAs) targeting all seven 23S rRNA genes (*rrlA*, *B*, *C*, *D*, *E*, *G*, and *H;* 7 *rrl* sgRNA) or only *rrlB*, *E*, and *G* (3 *rrl* sgRNA). In addition, we tested as negative controls two sgRNAs (*ctrl1* and *ctrl2*) without complementarity to the *E. coli* genome[25]. Combined downregulation of the seven *rrn* operons was not compatible with growth (Extended Data Fig. 7b). In the absence of (p)ppGpp, downregulation of the *rrnB*, *E*, and *G* operons resulted in ceftriaxone resistance (in conditions

of induction of *ycbB*; Fig. 4b and 4c) and to mecillinam resistance in the absence of *ycbB* induction (Extended Data Fig. 7c). The control sgRNAs had no phenotypic effect. A quantitative mass spectrometric analysis of ribosomal proteins was designed to determine whether CRISPRi-mediated downregulation of the distal portion of the *rrnB*, *E*, and *G* operons by the *3 rrl* sgRNA was resulting in a modification of the number of ribosomes per cell (Extended Data Fig. 8). The analysis of 188 unique tryptic fragments belonging to 49 ribosomal proteins indicated that 3 *rrl*-mediated CRISPR interference resulted in a minor (15%) but significant reduction in the number of ribosomes per cells (p-value < 0.0001). As a control, we sequenced the genome of the strain producing the *3 rrl* guide. This analysis revealed the presence of an unexpected mutation causing the $P^{376}R$ substitution in the β subunit of the RNAP. To evaluate whether the $P^{376}R$ substitution contributed to β-lactam resistance, we independently introduced plasmids pKT2(*ycbB*) and pHV136(*dcas9*; 3 *rrl*) in six sub-cultures of the BW25113 Δ*relA* Δ*spoT* strain whose genome was re-sequenced to eliminate the possible presence of any undesired mutation. The number of cultures required for the introduction of plasmids pKT2(*ycbB*) and pHV136(*dcas9*; 3 *rrl*) in this (p)ppGpp^0 strain and for the drug susceptibility assay was minimized. Under such conditions, induction of the genes encoding dCas9 and YcbB, in combination with constitutive transcription of the 3 *rrl* sgRNA, did not confer resistance to any of the six independently-constructed BW25113 Δ*relA* Δ*spoT* pKT2(*ycbB*) pHV136(*dcas9*; 3 *rrl*) strains (Extended Data Fig. 9). Thus β-lactam resistance depended upon both CRISPRi-mediated downregulation of *rrn* operons and the $P^{376}R$ substitution in the β subunit of the RNAP.

DISCUSSION

We used a trial-and-error strategy for elucidating the mechanism underlying the contribution of (p)ppGpp to β-lactam resistance, which has remained enigmatic for three decades. We first showed that the alarmone has no direct impact on peptidoglycan structure, including the proportion of 3→3 and 4→3 cross-links (Fig. 2 and Extended Data Fig. 2). This observation indicates that the contribution of (p)ppGpp to β-lactam resistance does not depend upon a modulation of the activity of peptidoglycan synthesis enzymes. Then, we established that a (p)ppGpp-mediated increase in the generation time is unlikely to account for the role of the alarmone in resistance. This conclusion was reached by showing that derivatives of a (p)ppGpp^0 strain remain susceptible to β-lactams in spite of increases in the generation time

resulting from (i) the production of RNAP with the Gln^{148}Leu, Gln^{148}Arg, Leu^{149}Arg, or Ile^{572}Leu substitutions in the β-subunit (Fig. 3), (ii) the exposure to sub-inhibitory concentrations of chloramphenicol, or (iii) a reduction of the growth temperature from 37 °C to 28 °C (Extended Data Fig. 6). The possibility that (p)ppGpp could bind to enzymes and directly modulate their catalytic activity was dismissed based on selection of RNAP mutants and overexpression of DksA, which both bypassed the requirement of the alarmone for resistance (Fig. 3, Extended Data Fig. 3). This result prompted us to investigate the mechanisms by which a modulation of the activity of the RNAP by (p)ppGpp could contribute to β-lactam resistance. First, we showed that the deletion or the overexpression of genes encoding alternative sigma factors did not affect the expression of β-lactam resistance (Extended Data Table 1). This observation indicates that the role of (p)ppGpp in resistance is unlikely to involve a modulation of specific genes that are expressed under the control of the alternative sigma factors. We then evaluated the contribution of a negative control of rRNA gene transcription to β-lactam resistance and showed that downregulation of three of the seven rRNA operons by CRISPR interference contributed to β-lactam resistance in the absence of (p)ppGpp (Fig. 4 and Extended Data Fig. 7). The *rrnB*, *E*, and *G* operons targeted by the 3 *rrl* sgRNA do not contain any distal tRNA genes downstream of the 5S rRNA gene. Thus, CRISPR interference mediated by the 3 *rrl* sgRNA could only result in decreased transcription of the 23S genes (directly targeted by the 3 *rrl* sgRNA) and the distal 5S rRNA genes in the same operons. The fact that the number of ribosomes per cell was only reduced by 15% (Extended Data Fig. 8), whereas the 3 *rrl* sgRNA targeted three of the seven operons (43%), implies that the negative control of the transcription of the *rrnB*, *E*, and *G* operons may be compensated by an increase in the transcription of the remaining operons (*rrnA*, *C*, *D*, and *H*). Such a compensatory mechanism has also been reported for deletions of one to four of the seven *rrn* operons of *E. coli* [26,27]. Strikingly, the reduction of the number of ribosomes resulting from the downregulation of three *rrn* operons in our study (15%) is similar to the reduction in the rRNA cell content (12%) previously reported for the deletion of three of the seven *rrn* operons[27]. Since the downregulation of the *rrnB*, *E*, and *G* operons was largely compensated by an increase in the transcription of the remaining operons, the contribution of downregulation of these operons to β-lactam resistance might not be quantitative in nature. A qualitative contribution instead might involve a depletion of the content of ribosomes in the specific 23S and 5S ribosomal RNAs encoded by the distal portion of the *rrnB*, *E*, and *G* operons. This hypothesis provokingly

implies that *E. coli* produces ribosomes that are functionally specialized depending upon their content in specific rRNAs. Alternatively, the moderate decrease in the number of ribosomes could account for resistance in combination with a pleiotropic effect of the $P^{376}R$ substitution, which disorganizes the gate-loop of the RNAP β subunit and could result in the destabilization of the open complex[28].

Strikingly, overproduction of (p)ppGpp had no impact on peptidoglycan structure (Fig. 2) indicating that the alarmone does not act by preventing binding of β-lactams to their PBP targets or by compensating for impaired D,D-transpeptidase activity of the PBPs. Instead, (p)ppGpp is likely to act by mitigating the consequences of PBP inactivation by β-lactams. The most recent model for the mechanism of bacterial killing by β-lactams[29–36] proposes that inhibition of D,D-transpeptidases by these drugs uncouples the transglycosylation and cross-linking reactions resulting in an energy-depleting futile cycle of peptidoglycan synthesis and degradation. This is associated with a dysregulation of the energy metabolism and increased protein synthesis, which ultimately leads to bacterial death due to the production of reactive oxygen species[32,35]. In agreement with this model, we observed in no instance a dissociation between the narrow-spectrum mecillinam resistance phenotype and the broad-spectrum β-lactam resistance phenotype conveyed by YcbB that involves distinct PBP targets. Furthermore, this model provides a rational explanation for the double requirement of YcbB and (p)ppGpp for β-lactam resistance as YcbB compensates for the loss of the transpeptidase activity of PBPs whereas (p)ppGpp protects the bacterium from the downstream effects of PBP inactivation by β-lactams. This model also accounts for the fact that production of (p)ppGpp is, in itself, sufficient for mecillinam resistance since the alarmone mitigates the deadly consequences of inactivation of the D,D-transpeptidase activity of PBP2, a β-lactam target specifically inactivated by mecillinam.

MATERIALS AND METHODS

Strains, plasmids, and growth conditions. The characteristics and origin of plasmids and strains used in the study are listed in Supplementary Table S1. Bacteria were grown at 37 °C in brain heart infusion (BHI; Difco) agar or broth with aeration (180 rpm). Kanamycin at 50 μg/ml was used for selection of transductants carrying the Km^R cassette obtained from the Keio collection[37]. The growth media were systemically supplemented with drugs to counter-select plasmid loss: 10

μg/ml tetracycline for vector pHV6 and derivatives, 20 μg/ml chloramphenicol for pHV7, pFR56, and derivatives, 25 μg/ml zeocin for pHV63zeo. Induction of the P_{trc}, P_{araBAD}, and P_{hlf} promoters was performed with isopropyl β-D-1-thiogalactopyranoside (IPTG), L-arabinose, and 2,4-diacetylphloroglucinol (DAPG), respectively. Plasmids constructed in this study were obtained by using NEBuilder HiFi DNA assembly (New England Biolabs) method, unless otherwise specified. Deletions of specific genes were obtained by P1 transduction of the Km^R cassette of selected mutants from the Keio collection[37,38]. For multiple gene deletions, the Km^R cassette was removed by the FLT recombinase encoded by plasmid pCP20.

Preparation of sacculi. Strains BW25113 Δ*relA* or BW25113 Δ*relA* Δ*ycbB* harboring plasmids pHV6 and pHV7 (vectors), pKT2(*ycbB*) and pHV7, pHV6 and pKT8(*relA'*), or pKT2(*ycbB*) and pKT8(*relA'*) were grown in BHI broth in the presence of 40 μM IPTG for induction of the P_{trc} promoter of pHV6 and pKT2(*ycbB*) and of 1% L-arabinose for induction of the P_{araBAD} promoter of pHV7 and pKT8(*relA*'). pHV6 and pHV7 are the vectors used for construction of pKT2(*ycbB*) and pKT8(*relA*'), respectively. The growth media contained tetracycline (to counterselect loss of pHV6 or pKT2) and chloramphenicol (to counterselect loss of pHV7 or pKT8). Bacteria were grown to late growth phase*, i.e.* to an OD_{600nm} greater than 1.0 (*ca*. 6 h at 37 °C under agitation). Ten μl of the resulting bacterial suspensions were platted on BHI agar supplemented with the same inducers (40 μM IPTG and 1% L-arabinose) and drugs (10 μg/ml tetracycline and 20 μg/ml chloramphenicol). For each replicate, 5 BHI agar plates were used in order to obtain a sufficient amount of bacteria. Plates were incubated for 16 h at 37 °C. Bacteria were harvested in two steps by scrapping each plate with 1 ml of phosphate-buffered saline (PBS) pH 7.2 followed by washing the plate with an additional 1 ml of PBS. Bacteria were boiled in 0.5 x PBS supplemented with 4% sodium dodecyl sulfate (SDS) in a final volume of 20 ml for 1 h. Sacculi were harvested by centrifugation (20,000 x *g* for 20 min at 20 °C), washed five times with 20 ml of water, resuspended in 1 ml of 20 mM Tris-HCl pH 7.5, and incubated with 100 μg/ml pronase at 37 °C for 16 h. Sacculi were washed five times with 1 ml of water, resuspended in 1 ml of 20 mM sodium phosphate pH 8.0 and incubated with 100 μg/ml trypsin at 37 °C for 16 h. Sacculi were washed five times with 1 ml of water, boiled for 5 min, collected by centrifugation, resuspended in 300 μl of water, and stored at -20 °C.

Peptidoglycan analysis. Ten μl of purified sacculi were digested with 120 μM lysozyme in 40 mM Tris-HCl pH 8.0 at 37 °C for 16 h. Insoluble material was removed by centrifugation at 12,000 rpm

in a microcentrifuge for 10 min and the soluble fraction containing muropeptides was reduced with sodium borohydride in 125 mM borate buffer pH 9.0 for 1 h at room temperature. Phosphoric acid was used to adjust the pH to 4.0. Muropeptides were separated by *rp*HPLC in a C18 column (Hypersil GOLD aQ; 250 x 4.6 mm; 3 µm, Thermo Scientific) at a flow rate of 1 ml/min with a linear gradient (0 to 20%) applied between 10 and 60 min (buffer A, TFA 0.1%; buffer B, acetonitrile 99.9%, TFA 0.1%, v/v). Absorbance was monitored at 205 nm and fractions were collected, lyophilized, resuspended in water, and analyzed by mass spectrometry. Mass spectra were obtained on a Bruker Daltonics maXis high-resolution mass spectrometer (Bremen, Germany) operating in the positive mode (Analytical Platform of the Muséum National d'Histoire Naturelle, Paris, France). Mass spectral data were explored using mineXpert2[39].

Mutant selection and phenotype analysis. *E. coli* BW25113 Δ*relA* Δ*spoT* pJEH12(*ycbB*) was streaked for isolated colonies on agar plates containing 10 µg/ml tetracycline to counter-select loss of plasmid pJEH12(*ycbB*). The selection procedure was independently carried out starting with independent colonies. Briefly, a fresh colony of *E. coli* BW25113 Δ*relA* Δ*spoT* pJEH12(*ycbB*) was inoculated in 5 ml of BHI broth supplemented with 10 µg/ml tetracycline. Bacteria were grown overnight at 37 °C with shaking (180 rpm). One hundred µl of overnight cultures were plated on BHI agar supplemented with 32 µg/ml ampicillin and 50 µM IPTG, 50 µg/ml mecillinam, or 16 µg/ml rifampicin. Plates were incubated overnight at 37 °C. The frequency of mutants was determined by dividing the number of CFUs obtained on the selective media by the total number of CFUs plated on the selective media. Each mutant presented in this work originates from independent experiments. Activation of YcbB-mediated β-lactam resistance in the mutants was confirmed using the disk diffusion assay in BHI agar supplemented or not with 50 µM IPTG to confirm that induction of *ycbB* was required for resistance[7]. Resistance to tetracycline and imipenem was also tested to confirm the presence of plasmid pJEH12(*ycbB*) and the dependence upon active YcbB, respectively. Disks were loaded with 10 µg of mecillinam, 10 µg of ampicillin, 30 µg of ceftriaxone, 10 µg of imipenem, 30 µg of tetracycline or 30 µg of rifampicin.

Whole-genome sequencing. To identify the mutations, 5 ml of BHI broth containing 10 µg/ml tetracycline were inoculated with a single colony of each selected mutants and genomic DNA was extracted (Wizard DNA extraction kit, Promega). Genomic DNA was either sequenced by paired-end joining Illumina (Novogene) or used for PCR amplification of the *rpoB* gene

followed by Sanger sequencing. For Illumina sequencing, paired-end reads of 150 bp were generated using a NovaSeq6000 (> 50x coverage). Read processing and identification of the mutations were performed with the *breseq* pipeline (v0.35.5)[40]. The positions of the mutations identified in the RNAP subunits are shown on the structures deposited on the Protein Data Bank [entry 5VSW (RNAP, DksA and ppGpp complex), 5UAC (RNAP and rifampicin complex), and 7KHV (RNAP and *rrnB* P1 promoter open complex)] using the PyMOL software (v2.3.4). Subunits of the structures were colored as indicated in the legends of the corresponding figures.

Determination of generation time. For each mutant tested, a fresh colony was inoculated in 1 ml BHI broth. Fifty µl of the suspension were inoculated in 150 µl BHI broth in 5 wells of 96-well plates. Incubation was performed at 37 °C overnight with agitation. Optical density at 600 nm was continuously determined with a plate-reader (Tecan Infinite 200 pro). For technical and biological replicates as detailed in legends, the generation time (G) was determined using the formula $G = \ln(\mu) / 2$, where µ corresponds to the slope of the linear part of the curved obtained by plotting the $\ln(OD_{600nm})$ as a function of time.

Plating efficiency assay. Bacteria were grown to late growth phase, *i.e.* to an OD_{600nm} greater than 1.0 (*ca*. 6 h at 37 °C under agitation). The OD_{600nm} was adjusted to 1.0 and 10-fold dilutions (10^{-1} to 10^{-5}) were prepared in BHI broth. Five µl of the resulting bacterial suspensions were spotted on BHI agar plates supplemented with inducers and drugs as indicated in the legend to figures. Plates were imaged after 16 h (or 24 h for plates containing ceftriaxone) of incubation at 37 °C. Data shown in the figures are representatives of at least two biological repeats.

Identification of genes that bypass the requirement of (p)ppGpp. To identify genes whose overexpression might bypass the requirement of (p)ppGpp in YcbB-mediated β-lactam resistance or mecillinam resistance, the pool of plasmids from the ASKA library[16,41] was transformed into BW25113 Δ*relA* Δ*spoT* pHV63zeo(*ycbB*). The resulting bacterial suspension was plated on BHI agar supplemented with 8 µg/ml ceftriaxone plus 1% L-arabinose to induce expression of *ycbB*, or 50 µg/ml mecillinam, and in the absence or presence of 20, 60, and 180 µM IPTG to induce expression of the ASKA plasmid-encoded genes. The media contained chloramphenicol to counter-select loss of the ASKA plasmids. Plates were incubated overnight at 37 °C. Twenty transformants selected with ceftriaxone plus L-arabinose and 20

transformants selected with mecillinam were isolated and their resistance phenotype confirmed. ASKA plasmids that produced resistant clones under the selective pressure of β-lactams were extracted and Sanger sequencing revealed in all 40 transformants the presence of the ASKA plasmid carrying the *dksA* gene.

Downregulation of *rrn* operons by CRISPRi. The options for choosing the RNA guide targeting a subset of the *rrn* operons were limited by: (i) the presence of a polymorphism common to a subset of the *rrn* operons; (ii) the presence of the polymorphism in the protospacer adjacent motif (PAM) to avoid off-target effects; (iii) the targeting of the 23S rRNA genes to avoid any effect on the tRNA genes located between the 16S and 23S rRNA genes; and (iv) the targeting of *rrn* operons that do not contain any tRNA genes at the 3' end of the operons (i.e. downstream of the distal 5S RNA genes). According to these four criteria, targeting of the *rrnB*, *E*, and *G* was the unique solution. The sgRNAs were under the control of the constitutive promoter of plasmid pFR56, which also mediates DAPG-inducible production of dCas9.

Ribosome preparation and analysis. *E. coli* BW25113 Δ*relA* Δ*spoT* harboring plasmids pKT2(*ycbB*) and derivatives of pFR56 encoding dCas9 and either the *ctrl1* or 3 *rrl* single-guide RNAs (sgRNAs) were grown overnight at 37 °C in 10 mL of BHI broth containing 10 µg/mL tetracycline and 20 µg/mL chloramphenicol under vigorous shaking. Two mL of this preculture were used to inoculate four Erlen-Meyer flasks containing 200 mL of BHI broth supplemented with 10 µg/mL tetracycline, 20 µg/mL chloramphenicol, 40 µM IPTG for induction of *ycbB*, and 50 µM DAPG for induction of *dcas9*. Cells were grown at 37 °C under vigorous shaking to an optical density at 600 nm (OD_{600}) of 0.6 (average of 0.607 ± 0.123 *versus* 0.619 ± 0.073 for the *ctrl1* and 3 *rrl* cultures, respectively, n = 4 for each strain). Thirty mL of each culture were centrifuged (5,000 x *g* at 4 °C for 8 min), harvested bacteria were washed twice with 30 mL of cold PBS, and the pellet was frozen in liquid nitrogen. To obtain fully labeled cells, *E. coli* BW25113 was grown in 500 mL of M9 minimal medium containing 0.2% ^{13}C D-glucose and ^{15}N ammonium chloride (Eurisotop) at 37 °C under vigorous shaking to an OD_{600} of 1.0. Cells were harvested by centrifugation (5,000 x *g* at 4 °C for 8 min), washed twice with 30 mL of cold PBS, and resuspended in 25 mL of ribosome lysis buffer (RLB; 50 mM Tris-HCl pH 7.5, 50 mM magnesium acetate, 100 mM ammonium chloride, 1 mM DTT, and 0.5 mM EDTA), and frozen in liquid nitrogen. An aliquot of 1 mL (equivalent of 20 mL of culture) of labeled cells was used to resuspend the bacterial pellets corresponding to 30 mL of each one of the four unlabeled

cultures. The resulting bacterial suspensions were sonicated on ice (3 x 30 s). Lysates were clarified by centrifugation (20,000 x *g* at 4 °C for 20 min). The clarified lysates were deposited on top of 30 mL of a 1.1 M saccharose solution in ribosome lysis buffer. Ribosomes were pelleted (100,000 x *g* overnight at 4 °C) in a fixed angle rotor and resuspended in 300 µL of 100 mM ammonium acetate buffer pH 7.5, distributed in four aliquots of 75 µL, and frozen in liquid nitrogen.

Identification of the purified proteins and quantification of the tryptic fragments was performed by liquid chromatography-mass spectrometry (LC-MS/MS). The ribosomal preparations (30 µL) were processed by subjecting them to a short-time SDS-polyacrylamide gel electrophoresis to let the proteins enter the stacking gel but not to get resolved. The gel band was excised and a third of it was sliced to perform the reduction-alkylation stem prior to the trypsin-based hydrolysis of the proteins. For each sample the peptidic content was estimated by measuring the absorbance at 280 nm. The sample volume was adjusted so that a volume of 4 µL of sample would carry 400 ng of peptides for injection into a nanoLC-Ultra system (Eksigent, Dublin, CA, USA). The chromatographic column was a Biosphere C18 (length: 31 cm, inner diameter: 75 µm, particle size: 3 µm, pore size: 120 Å). Chromatography was performed at a flow rate of 300 nL/min (buffer A: 99.9% water, 0.1% formic acid; buffer B: 99.9% acetonitrile, 0.1% formic acid). The chromatographic separation was run over 80 min with two gradient development steps (i) from 5 % to 30 % buffer B in 75 min and (ii) to 95 % buffer B in 5 min. The analytes eluting from the chromatographic column were injected in a Q ExactivePlus mass spectrometer (Thermo Scientific, Courtaboeuf, France) using a nano-electrospray interface and ionized using a liquid junction and an uncoated capillary probe (10 µm inner diameter; New Objective, Woburn, MA, USA).

Full scan MS acquisition settings were as follows: resolution, 70,000; AGC target, 3×10^6; maximum ion time, 60 ms; scan range, 350-1400 *m*/*z*; acquisition type, profile. Data dependent MS/MS acquisition settings were as follows: resolution, 17,500; AGC target, 10^5; maximum ion time, 120 ms; topN, 8; isolation window, 1.5 *m*/*z*; normalized collision energy, 27%; acquisition type, profile. The mass spectrometer was directed (i) to select ions of charge state either 2+ or 3+ showing an expected isotopic pattern for unlabeled peptide, (ii) to exclude secondary isotopic peaks, and (iii) to exclude already fragmented ions for 50 s.

A standard bottom-up proteomics approach yielded ribosomal protein identifications based on the unlabeled peptides contained in each sample. The identification and quantification processes were carried out using an updated version of the i2MassChroQ (the preferred software version for this work is 1.0.0)[42,43]. By using the elemental composition of each identified unlabeled peptide ion (along with its charge restricted to $z = 2$), the m/z value of the fully labeled peptide ion counterpart was computed. The (rt, m/z, z) triplets of the labeled and unlabeled ions eluting at the same retention time (rt) were used to perform ion current extractions (an area-under-the-curve measurement). Further data processing was restricted to peptides from ribosomal proteins having identified light and heavy isotopologues in all eight samples corresponding to the four biological repeats for both the *ctrl1* and 3 *rrl* sgRNAs. For each peptide found in all eight samples, the ratio of the unlabeled to labeled ion peak areas (light-to-heavy-area ratio) was computed. The mean value ($\bar{x}$) of the light-to-heavy-area ratio measurements was computed separately in each group (*ctrl1* and 3 *rrl* samples). The identified peptides in the *ctrl1* and 3 *rrl* groups that have any one of the four light-to-heavy-area ratios outside of the $[0.5 < \bar{x} < 2]$ interval were filtered out of the data set.

Statistics and reproducibility. For the plating efficiency assays, at least two biological repeats were performed. For peptidoglycan analysis by *rp*HPLC and mass spectrometry, three independent biological repeats were performed. Antibiotic susceptibility testing data are medians from three independent biological repeats. Generation time was determined from at least three biological repeats. For proteomic analysis of ribosome content, four independent biological repeats were performed. The light-to-heavy mean ratios of 188 unique tryptic fragments belonging to 49 ribosomal proteins were compared between the two conditions, and the p-value (< 0.0001) was obtained from unpaired two-tailed t-test using Welch's correction for heteroscedasticity.

ACKNOWLEDGEMENTS

This work was supported by the French National Research Agency ANR 'RegOPeps' (grant ANR-19-CE44-0007 to JEH). HV and CAP are the recipients of doctoral fellowships from Sorbonne-Université (ED 515, Complexité du Vivant). We thank A. Marie for technical assistance in the collection of mass spectra at the Plateau Technique de Spectrométrie de Masse Bio-Organique

of the Muséum national d'Histoire Naturelle. We thank E. Maisonneuve for the kind gift of the pool of the ASKA plasmids. We thank Z. Edoo for proof-reading the manuscript.

AUTHOR CONTRIBUTIONS

HV: conception and design; acquisition, analysis, and interpretation of data; drafting and revising the article. CAP: conception and design; acquisition, analysis, and interpretation of data; revising the article. FR and OL: mass spectrometric analysis of ribosome preparations and quantitative mass data processing. JEH and MA: conception and design; analysis and interpretation of data; drafting and revising the article.

CONFLICT OF INTEREST

The authors declare that there is no conflict of interest.

DATA AVAILABILITY

Source data are provided with this paper. Whole genome sequencing raw data of RNAP mutants are available at the Sequence Read Archive database (SRA) under accession code PRJNA1044113.

CODE AVAILABILITY

The i2MassChroQ software used to identify and quantify the tryptic peptides is freely available at https://forgemia.inra.fr/pappso/i2masschroq/-/releases (the preferred software version for this work is 1.0.0).

REFERENCES

1. Hauryliuk, V., Atkinson, G. C., Murakami, K. S., Tenson, T. & Gerdes, K. Recent functional insights into the role of (p)ppGpp in bacterial physiology. *Nat. Rev. Microbiol.* **13**, 298–309 (2015).

2. Irving, S. E., Choudhury, N. R. & Corrigan, R. M. The stringent response and physiological roles of (pp)pGpp in bacteria. *Nat. Rev. Microbiol. 2020 194* **19**, 256–271 (2020).

3. Zhang, Y., Zborníková, E., Rejman, D. & Gerdes, K. Novel (p)ppGpp Binding and Metabolizing Proteins of Escherichia coli. *MBio* **9**, (2018).

4. Sanchez-Vazquez, P., Dewey, C. N., Kitten, N., Ross, W. & Gourse, R. L. Genome-wide effects on Escherichia coli transcription from ppGpp binding to its two sites on RNA polymerase. *Proc. Natl. Acad. Sci.* **116**, 8310–8319 (2019).

5. Garde, S., Chodisetti, P. K. & Reddy, M. Peptidoglycan: Structure, Synthesis, and Regulation. *EcoSal Plus* **9**, (2021).

6. Mainardi, J. L. *et al.* A novel peptidoglycan cross-linking enzyme for a β-lactam-resistant transpeptidation pathway. *J. Biol. Chem.* **280**, 38146–38152 (2005).

7. Hugonnet, J. E. *et al.* Factors essential for L,D-transpeptidase-mediated peptidoglycan cross-linking and β-lactam resistance in Escherichia coli. *Elife* **5**, (2016).

8. Vinella, D., D'Ari, R. & Bouloc, P. Penicillin binding protein 2 is dispensable in Escherichia coli when ppGpp synthesis is induced. *EMBO J.* **11**, 1493–1501 (1992).

9. Trinh, V., Langelier, M.-F., Archambault, J. & Coulombe, B. Structural Perspective on Mutations Affecting the Function of Multisubunit RNA Polymerases. *Microbiol. Mol. Biol. Rev.* **70**, 12–36 (2006).

10. Patel, Y., Soni, V., Rhee, K. Y. & Helmann, J. D. Mutations in rpoB That Confer Rifampicin Resistance Can Alter Levels of Peptidoglycan Precursors and Affect β-Lactam Susceptibility. *MBio* **14**, (2023).

11. Ross, W. *et al.* ppGpp Binding to a Site at the RNAP-DksA Interface Accounts for Its Dramatic Effects on Transcription Initiation during the Stringent Response. *Mol. Cell* **62**, 811–823 (2016).

12. Myers, A. R., Thistle, D. P., Ross, W. & Gourse, R. L. Guanosine Tetraphosphate Has a Similar Affinity for Each of Its Two Binding Sites on Escherichia coli RNA Polymerase. *Front. Microbiol.* **11**, 587098 (2020).

13. Paul, B. J. *et al.* DksA: A critical component of the transcription initiation machinery that potentiates the regulation of rRNA promoters by ppGpp and the initiating NTP. *Cell* **118**, 311–322 (2004).

14. Paul, B. J., Berkmen, M. B. & Gourse, R. L. DksA potentiates direct activation of amino acid promoters by ppGpp. *Proc. Natl. Acad. Sci. U. S. A.* **102**, 7823–7828 (2005).

15. Potrykus, K., Murphy, H., Philippe, N. & Cashel, M. ppGpp is the major source of growth rate control in E. coli. *Environ. Microbiol.* **13**, 563 (2011).

16. Kitagawa, M. *et al.* Complete set of ORF clones of Escherichia coli ASKA library (a complete set of E. coli K-12 ORF archive): unique resources for biological research. *DNA Res.* **12**, 291–299 (2005).

17. Sharma, U. K. & Chatterji, D. Transcriptional switching in Escherichia coli during stress and starvation by modulation of sigma activity. *FEMS Microbiol. Rev.* **34**, 646–657 (2010).

18. Mauri, M. & Klumpp, S. A Model for Sigma Factor Competition in Bacterial Cells. *PLoS Comput. Biol.* **10**, e1003845 (2014).

19. Dartigalongue, C., Missiakas, D. & Raina, S. Characterization of the Escherichia coli σE Regulon. *J. Biol. Chem.* **276**, 20866–20875 (2001).

20. Zhao, K., Liu, M. & Burgess, R. R. The Global Transcriptional Response of Escherichia coli to Induced σ32 Protein Involves σ32 Regulon Activation Followed by Inactivation and Degradation of σ32 in Vivo. *J. Biol. Chem.* **280**, 17758–17768 (2005).

21. Nonaka, G., Blankschien, M., Herman, C., Gross, C. A. & Rhodius, V. A. Regulon and promoter analysis of the E. coli heat-shock factor, σ32, reveals a multifaceted cellular response to heat stress. *Genes Dev.* **20**, 1776 (2006).

22. Potrykus, K. *et al.* Antagonistic Regulation of Escherichia coli Ribosomal RNA rrnB P1 Promoter Activity by GreA and DksA. *J. Biol. Chem.* **281**, 15238–15248 (2006).

23. Magnusson, L. U., Gummesson, B., Joksimović, P., Farewell, A. & Nyström, T. Identical, independent, and opposing roles of ppGpp and DksA in Escherichia coli. *J. Bacteriol.* **189**, 5193–5202 (2007).

24. Qi, L. S. *et al.* Repurposing CRISPR as an RNA-γuided platform for sequence-specific control of gene expression. *Cell* **152**, 1173–1183 (2013).

25. Rousset, F. *et al.* The impact of genetic diversity on gene essentiality within the Escherichia coli species. *Nat. Microbiol. 2021 63* **6**, 301–312 (2021).

26. Condon, C., French, S., Squires, C. & Squires, C. L. Depletion of functional ribosomal RNA operons in Escherichia coli causes increased expression of the remaining intact copies. *EMBO J.* **12**, 4305 (1993).

27. Fleurier, S., Dapa, T., Tenaillon, O., Condon, C. & Matic, I. rRNA operon multiplicity as a bacterial genome stability insurance policy. *Nucleic Acids Res.* **50**, 12601 (2022).

28. Mazumdar, M. N. *et al.* RNA polymerase gate loop guides the nontemplate DNA strand in transcription complexes. *Proc. Natl. Acad. Sci. U. S. A.* **113**, 14994–14999 (2016).

29. Cho, H., Uehara, T. & Bernhardt, T. G. Beta-Lactam Antibiotics Induce a Lethal Malfunctioning of the Bacterial Cell Wall Synthesis Machinery. *Cell* **159**, 1300–1311 (2014).

30. Dwyer, D. J. *et al.* Antibiotics induce redox-related physiological alterations as part of their lethality. *Proc. Natl. Acad. Sci.* **111**, E2100–E2109 (2014).

31. Foti, J. J., Devadoss, B., Winkler, J. A., Collins, J. J. & Walker, G. C. Oxidation of the guanine nucleotide pool underlies cell death by bactericidal antibiotics. *Science (80-.).* **336**, 315–319 (2012).

32. Kawai, Y. *et al.* Crucial role for central carbon metabolism in the bacterial L-form switch and killing by β-lactam antibiotics. *Nat. Microbiol. 2019 410* **4**, 1716–1726 (2019).

33. Kohanski, M. A., Dwyer, D. J., Hayete, B., Lawrence, C. A. & Collins, J. J. A Common Mechanism of Cellular Death Induced by Bactericidal Antibiotics. *Cell* **130**, 797–810 (2007).

34. Lobritz, M. A. *et al.* Antibiotic efficacy is linked to bacterial cellular respiration. *Proc. Natl. Acad. Sci. U. S. A.* **112**, 8173–8180 (2015).

609 35. Lobritz, M. A. *et al.* Increased energy demand from anabolic-catabolic processes
610 drives β-lactam antibiotic lethality. *Cell Chem. Biol.* **29**, 276-286.e4 (2022).

611 36. Voedts, H., Kennedy, S. P., Sezonov, G., Arthur, M. & Hugonnet, J. E. Genome-wide
612 identification of genes required for alternative peptidoglycan cross-linking in
613 Escherichia coli revealed unexpected impacts of β-lactams. *Nat. Commun. 2022 131*
614 **13**, 1–14 (2022).

615 37. Baba, T. *et al.* Construction of *Escherichia coli* K-12 in-frame, single-gene knockout
616 mutants: the Keio collection. *Mol. Syst. Biol.* **2**, (2006).

617 38. Datsenko, K. A. & Wanner, B. L. One-step inactivation of chromosomal genes in
618 Escherichia coli K-12 using PCR products. *Proc. Natl. Acad. Sci. U. S. A.* **97**, 6640–6645
619 (2000).

620 39. Langella, O. & Rusconi, F. mineXpert2: Full-Depth Visualization and Exploration of MS
621 n Mass Spectrometry Data. *J. Am. Soc. Mass Spectrom.* **32**, 1138–1141 (2021).

622 40. Deatherage, D. E. & Barrick, J. E. Identification of mutations in laboratory-evolved
623 microbes from next-generation sequencing data using breseq. *Methods Mol. Biol.*
624 **1151**, 165–188 (2014).

625 41. Germain, E. *et al.* YtfK activates the stringent response by triggering the alarmone
626 synthetase SpoT in Escherichia coli. *Nat. Commun. 2019 101* **10**, 1–12 (2019).

627 42. Valot, B., Langella, O., Nano, E. & Zivy, M. MassChroQ: a versatile tool for mass
628 spectrometry quantification. *Proteomics* **11**, 3572–3577 (2011).

629 43. Langella, O. *et al.* X!TandemPipeline: A Tool to Manage Sequence Redundancy for
630 Protein Inference and Phosphosite Identification. *J. Proteome Res.* **16**, 494–503
631 (2017).

632 44. Potrykus, K. & Cashel, M. Stringent Mutant/Stringent Response. in *Brenner's*
633 *Encyclopedia of Genetics: Second Edition* 570–572 (Elsevier Inc., 2013).
634 doi:10.1016/B978-0-12-374984-0.01485-6.

635 45. Voedts, H. *et al.* Role of endopeptidases in peptidoglycan synthesis mediated by
636 alternative cross-linking enzymes in Escherichia coli. *EMBO J.* **40**, e108126 (2021).

Figure 1. Pleiotropic effects of (p)ppGpp in *E. coli*. The (p)ppGpp alarmone binds to enzymes involved in multiple metabolic pathways, such as the GuaB inosine monophosphate dehydrogenase, the DnaG DNA primase, and the PPX polyphosphate kinase[3]. The alarmone also modulates the expression of approximatively 1200 genes by binding to two sites on RNA polymerase (RNAP)[4]. Modulation of gene expression involves (1) activation of specific promoters involved in amino acid synthesis, (2) recruitment of alternative sigma factors, and (3) downregulation of ribosomal RNA operons[2,17].

Figure 2. Impact of (p)ppGpp and YcbB production on peptidoglycan structure. (**a**) Representative *rp*HPLC profiles of muropeptides from strains BW25113 Δ*relA* harboring vectors pHV6 and pHV7 (grey) or pHV6 and plasmid pKT8(*relA'*) (dark red). (**b**) Representative *rp*HPLC profiles of muropeptides from strains BW25113 Δ*relA* harboring plasmids pKT2(*ycbB*) and pHV7 (grey) or pKT2(*ycbB*) and pKT8(*relA'*) (dark red). (**c**) Structure of the muropeptides eluted in *rp*HPLC peaks 1 to 10 deduced from mass spectrometry analyses. Tetra, tetrapeptide L-Ala-D-iGlu-DAP-D-Ala; Tri, tripeptide L-Ala-D-iGlu-DAP; Tri-KR, tripeptide L-Ala-D-iGlu-DAP substituted by the dipeptide Lys-Arg originating from the Braun lipoprotein; Tri-Tri and Tri-Tetra, dimers containing a tripeptide donor stem linked to a tripeptide or tetrapeptide acceptor stem, respectively. These dimers contained a 3→3 cross-link formed by the YcbB L,D-transpeptidase. Tetra-Tri and Tetra-Tetra, dimers containing a tetrapeptide donor linked to a tripeptide or tetrapeptide acceptor, respectively. These dimers contained a 4→3 cross-link formed by D,D-transpeptidases belonging to the PBP family. Tetra(Gly), Tri-Tetra(Gly), and Tetra-Tetra(Gly), muropeptides containing a Gly residue instead of D-Ala at the 4th position of the free stem. These muropeptides originated from the exchange of D-Ala by Gly catalyzed by L,D-transpeptidases. Data are representative chromatograms from three biological repeats. (**d**) Relative peak area of muropeptides extracted from strains BW25113 Δ*relA* harboring plasmids pHV6 and pHV7 (grey), pHV6 and pKT8(*relA'*) (dark red), pKT2(*ycbB*) and pHV7 (dashed grey), or pKT2(*ycbB*) and pKT8(*relA'*) (dashed dark red). Induction of *relA* had no impact on peptidoglycan structure in these strains (panel d) as well as in derivatives of the same strains lacking the chromosomal copy of *ycbB* (Extended Data Fig. 2). Data are means and standard deviations from three biological repeats (n = 3). Tri and Tetra, disaccharide-tripeptide and disaccharide-tetrapeptide monomers, respectively. 3→3 and 4→3, dimers containing 3→3 and 4→3 cross-links, respectively.

Figure 3. Localization of amino acid substitutions mediating β-lactam and rifampicin resistance in the RNAP holoenzyme. (**a**) Table of RNAP substitutions and the corresponding generation times (GT) of (p)ppGpp^0 mutants selected on media containing ampicillin plus IPTG (Amp), mecillinam (Mel), or rifampicin (Rif). ND, not determined. Note that the table includes 16 distinct amino acid substitutions including Arg^{451}Cys [due to the same mutation (CGT→TGT)] that was independently obtained on media containing ampicillin or mecillinam and Thr^{563}Pro (due to ACC→CCC) that was obtained on all three selectors. GT was determined from at least three biological repeats (n ≥ 3). (**b**) Cartoon and surface representations of the PDB entry 5VSW are shown with subunits highlighted in various colors. ppGpp molecules at the two binding sites of RNAP are indicated by red arrows and circles. The inset shows the localization of amino acid substitutions conferring resistance to β-lactams only (green), to rifampicin only (red), and to both β-lactams and rifampicin (yellow). Substitutions are localized in the β subunit (not indicated) or β' subunit (indicated in parentheses). The figure was generated with PyMOL (v2.3.4). See Potrykus, K. and Cashel, M. (2013)[44] for an exhaustive review of amino acid substitutions detected in RNAP subunits.

Figure 4. Impact of downregulation of rRNA transcription on β-lactam resistance. (**a**) Schematic representation of the CRISPR interference approach used to decrease expression of several *rrn* operons at once. The *rrnA* operon is displayed as an example. The catalytically inactive Cas9 (dCas9) associates to the single-guide RNA (sgRNA) and binds to the chromosomal target (a sequence within the 23S rRNA gene *rrlA*). The elongating RNAP that encounters dCas9 dissociates from the DNA matrix, leading to downregulation of the targeted gene. The rational design of the 3 *rrl* guide is described in the Extended Data Fig. 7a. (**b**) Plating efficiency of (i) the RpoB G^{449}V mutant harboring pKT2(*ycbB*) (positive control), (ii) the parental strain BW25113 Δ*relA* Δ*spoT* pKT2(*ycbB*) (negative control), and (iii) derivatives of the latter strain harboring plasmids encoding dCas9 under the control of the DAPG-inducible P_{hlf} promoter and one of the four sgRNAs expressed under the control of a constitutive promoter. The sgRNAs targeted seven (7 *rrl*) or three (3 *rrl*) of the seven 23S rRNA genes. The remaining sgRNAs, *ctrl1* and *ctrl2*, do not target any sequence in the *E. coli* chromosome[25]. P^{376}R*, genome re-sequencing identified a substitution (P^{376}R) in the β subunit of the RNAP in the strain expressing the 3 *rrl* sgRNA. Growth was tested in the presence of ceftriaxone at 8 µg/ml (+ ceftriaxone) or in the absence of the drug (- ceftriaxone). Induction of the *dcas9* gene was performed with 50 µM DAPG. BHI agar plates contained 40 µM IPTG for induction of *ycbB*. (**c**) Colony forming units (CFUs) were enumerated for the same strains and the same growth conditions by plating

100 µL of 10-fold dilutions on agar plates. The detection limit was 10^2 cfu/mL. Horizontal bars indicate the means from three biological repeats (n = 3).

Extended Data Figure 1. Reactions catalyzed by PBPs and L,D-transpeptidases. (**a**) Peptidoglycan cross-linking by PBPs is a two-step reaction initiated by the activation of the catalytic Ser residue for nucleophilic attack of the carbonyl of D-Ala^4 in a pentapeptide donor stem. This first step results in the release of D-Ala^5 and formation of an acyl-enzyme. In the second step, the carbonyl of the resulting ester bond undergoes nucleophilic attack by the side-chain amino group of the diaminopimelyl (DAP) residue of an acceptor. This results in the release of the PBP and in the formation a peptidoglycan dimer (Tetra→Tri or Tetra→Tetra) containing a 4→3 cross-link, which connects D-Ala at the 4th position of the donor to DAP at the 3rd position of the acceptor. Tetra→Tri and Tetra→Tetra dimers differ by the presence of a tripeptide or a tetrapeptide in the acceptor position, respectively. D,D-transpeptidase catalytic domains are found in Class A PBPs PBP1a, PBP1b, and PBP1c, which also contain a glycosyltransferase domain for glycan chain elongation. D,D-transpeptidase catalytic domains are also found in monofunctional Class B PBP2 and PBP3. (**b**) The L,D-transpeptidases YcbB (LdtD) and YnhG (LdtE) also catalyze peptidoglycan in a two-step reaction similar to that catalyzed by PBPs. Main differences involve the nature of (i) the nucleophile: a cysteine instead of a serine, (ii) the donor stem: a tetrapeptide instead of a pentapeptide, and (iii) the cross-link: 3→3 instead of 4→3.

Extended Data Figure 2. Impact of (p)ppGpp and YcbB production on peptidoglycan structure in strains lacking the chromosomal copy of *ycbB*. Relative peak area of muropeptides extracted from strains BW25113 Δ*relA* Δ*ycbB* harboring plasmids pHV6 and pHV7 (blue), pHV6 and pKT8(*relA'*) (orange), pKT2(*ycbB*) and pHV7 (dashed blue), or pKT2(*ycbB*) and pKT8(*relA'*) (dashed orange). Data are means and standard deviations from three biological repeats (n = 3). Tri and Tetra, disaccharide-tripeptide and disaccharide-tetrapeptide monomers, respectively. 3→3 and 4→3, dimers containing 3→3 and 4→3 cross-links, respectively.

Extended Data Figure 3. Position of the amino acid substitutions in the RNAP β subunit at the proximity of the rifampicin binding site (a) and DNA in the open promoter complex (b). Cartoon and surface representations of the PDB entry 5UAC (**a**) and 7KHB (**b**) are shown with subunits highlighted in various colors. (p)ppGpp binding sites of RNAP are indicated by red arrows and dashed circles. Substitutions led to resistance to β-lactams only (green), to rifampicin only (red), and to both β-lactams and rifampicin (yellow). The inset in panel (**a**) shows rifampicin (pink) bound to RNAP (for the sake of simplicity, only the β subunit is shown). The inset in panel (**b**) shows DNA (grey) of the *rrnB* P1 open promoter complex. All substitutions are localized in the β subunit except substitutions in positions 333, 1144, 1147, and 1308 of β' subunit (indicated in parentheses). The figure was generated with PyMOL (v2.3.4).

Extended Data Figure 4. Role of (p)ppGpp binding to the two RNAP binding sites. Plating efficiency of BW25113 Δ*relA* pKT2(*ycbB*) pKT8(*relA'*) and its derivatives obtained by deletion of the *rpoZ* or *dksA* genes. Growth was tested in the presence of ceftriaxone at 8 µg/ml (+ ceftriaxone) or in the absence of the drug (- ceftriaxone) on BHI agar plates supplemented with 40 µM IPTG and 1% L-arabinose for induction of *ycbB* and *relA'*, respectively (n = 3).

Extended Data Figure 5. Role of the Q^{148}L and G^{449}V RpoB substitutions in β-lactam and rifampicin resistance. Plating efficiency was performed for BW25113 Δ*relA* Δ*spoT* pKT2(*ycbB*) and its derivatives harboring mutations leading to the G^{449}V or Q^{148}L substitution in the β-subunit of the RNAP (encoded by *rpoB*). Growth was tested in BHI agar supplemented by the indicated antibiotics and 40 µM IPTG for induction of *ycbB*. DNA was extracted from the cultures that were used for the phenotypic analysis and whole genome sequencing did not reveal any additional mutation in the genes encoding the RNAP subunits. This control indicates that our analysis is not biased by the accumulation of suppressors of the Δ*relA* and Δ*spoT* mutations. Data are a representative of three independent experiments (n = 3).

Extended Data Figure 6. Impact of sub-inhibitory concentrations of chloramphenicol on the generation time and expression of ceftriaxone resistance. (**a**) Generation time (GT) as a function of supplementation of BHI broth with various concentrations of chloramphenicol. Each point is the median from five biological repeat. (**b**) Plating efficiency of the RpoB G^{449}V mutant harboring pKT2(*ycbB*) (positive control) and of the parental BW25113 Δ*relA* Δ*spoT* pKT2(*ycbB*) strain in the absence (- Cm) or presence (+ Cm) of chloramphenicol at various concentrations. All plates contained 40 µM IPTG for induction of *ycbB*. Plates contained 8 µg/ml ceftriaxone (+ ceftriaxone) or no

drug (- ceftriaxone). Data are a representative of five biological repeats. (**c**) Plating efficiency of the RpoB $G^{449}V$ mutant harboring pKT2(*ycbB*) (positive control) and of the parental BW25113 Δ*relA* Δ*spoT* pKT2(*ycbB*) strain grown at 28 °C. Plates contained 40 µM IPTG for induction of *ycbB*, 8 µg/ml ceftriaxone (+ ceftriaxone) or no drug (- ceftriaxone). Data are a representative of five biological repeats. The generation time of the parental strain was 38 ± 4 min at 28 °C *versus* 24 ± 1 min at 37 °C (determined from five biological repeats).

Extended Data Figure 7. Lowering rRNA transcription bypasses the requirement of (p)ppGpp for mecillinam resistance. (**a**) Sequence alignments of portions of the *rrl* genes targeted by the sgRNAs. Variable positions exploited to downregulate *rrlB, E, and G* without affecting *rrlA, C, D,* and *H* expression are marked by asterisks. sgRNA sequences shown are the reverse complements (RC) of the sgRNA sequences used to downregulate *rrl* transcription. See Material and Methods for the design of sgRNAs. (**b**) Plating efficiency of derivatives of BW25113 Δ*relA* Δ*spoT* harboring plasmids encoding dCas9 under the control of the DAPG-inducible P_{hlf} promoter and four sgRNAs under the control of a constitutive promoter. The sgRNAs targeted seven (7 *rrl*) or three (3 *rrl*) of the seven 23S rRNA genes. The remaining sgRNAs, *ctrl1* and *ctrl2*, do not target any sequence in the *E. coli* chromosome[25]. Induction of the *dcas9* gene was performed with 25, 50, or 200 µM DAPG. Induction of *dcas9* in the presence of the 7 *rrl* sgRNA prevented growth of BW25113 Δ*relA* Δ*spoT* at DAPG concentrations of 50 and 200 µM. Effective downregulation of all 7 *rrl* copies is likely to account for the absence of growth. (**c**) Plating efficiency of the RpoB $G^{449}V$ mutant (positive control), the parental strain BW25113 Δ*relA* Δ*spoT* pKT2(*ycbB*) (negative control) and its derivatives harboring plasmids encoding dCas9 under the control of the DAPG-inducible P_{hlf} promoter and the four sgRNAs under the control of a constitutive promoter. Growth was tested in the presence of mecillinam at 16 µg/ml (+ mecillinam) or in the absence of the drug (- mecillinam). Induction of the *dcas9* gene was performed with 50 µM DAPG. Mecillinam resistance was obtained in the absence of *ycbB* induction. Induction of the gene encoding dCas9 was associated with a 1.4-fold increase in the generation time (from 28 ± 2 min versus 37 ± 1 min; n = 3).

Extended Data Figure 8. Impact of the downregulation of *rrn* operons on the relative number of ribosomes per cell. (**a**) Unlabeled ribosomes were purified from derivatives of BW25113 Δ*relA* Δ*spoT* pKT2(*ycbB*) harboring pHV137(*dcas9*; *ctrl1*) or pHV136(*dcas9*; 3 *rrl*) (n = 4). Tet, 10 µg/mL tetracycline; Cm, 20 µg/mL chloramphenicol; RLB, Ribosome lysis buffer. 40 µM IPTG and 50 µM DAPG were used to induce expression of *ycbB* and *dcas9*, respectively. Labeled ribosomes were purified from BW25113. (**b**) Sample preparation and data acquisition. Ribosomes digested with trypsin were analyzed by LC-MS/MS. The representative full scan spectrum obtained for the VANLGSLGDQVNVK peptide of protein L9 shows the isotopic distributions for the unlabeled and labeled isotopologues. (**c**) Distribution of light-to-heavy mean ratios. The boxes extend from the 25th to 75th percentiles. The line in the middle of the box is plotted at the median. The whiskers extend from the 5th to 95th percentiles. Outliers (< 5% or > 95%) are represented outside of the box plot by circles and squares. ****, *p*-value < 0.0001 for comparison of the means; unpaired two-tailed *t*-test with Welch's correction for heteroscedasticity.

Extended Data Figure 9. Expression of ceftriaxone resistance mediated by downregulation of the transcription of *rrl* genes in the absence of the $P^{376}R$ substitution in the β subunit of the RNAP. Plating efficiency of the BW25113 Δ*relA* Δ*spoT* pKT2(*ycbB*) pHV136(*dcas9*; 3 *rrl*). The parental strain BW25113 Δ*relA* Δ*spoT* was re-sequenced to ensure the absence of mutations in the genes encoding the RNAP subunits. Plasmids pKT2(ycbB) and pHV136(*dcas9*; 3 *rrl*) plasmids were independently introduced in six independent cultures of this strain (clones 1 to 6). The strain appearing in the top row and in Fig. 4 additionally harbored the unexpected $P^{376}R$ substitution in the β subunit of the RNAP. Growth was tested in the presence of 8 µg/mL ceftriaxone (+ ceftriaxone), 16 µg/mL mecillinam (+ mecillinam), or in the absence of the drugs (- β-lactam). Induction of *dcas9* was performed with 50 µM DAPG (+ DAPG). BHI agar plates contained 40 µM IPTG for induction of *ycbB* (n = 6).

Extended Data Table 1. YcbB- and (p)ppGpp-mediated β-lactam resistance does not rely on the recruitment of a specific alternative sigma factor

Host / Plasmid	Inducers[b]	Inhibition zones (mm)[a] Mel	Amp	Cro
BW25113 Δ*relA*	None	20	18	34
pKT2(*ycbB*) pKT8(*relA'*)	IPTG + Ara	< 6	< 6	15
Deletion of genes encoding unessential alternative σ factors				
BW25113 Δ*relA* Δ*rpoN*				
pKT2(*ycbB*) pKT8(*relA'*)	IPTG + Ara	< 6	< 6	16
BW25113 Δ*relA* Δ*rpoS*				
pKT2(*ycbB*) pKT8(*relA'*)	IPTG + Ara	< 6	< 6	15
BW25113 Δ*relA* Δ*rpoF*				
pKT2(*ycbB*) pKT8(*relA'*)	IPTG + Ara	< 6	< 6	15
BW25113 Δ*relA* Δ*fecI*				
pKT2(*ycbB*) pKT8(*relA'*)	IPTG + Ara	< 6	< 6	14
Overexpression of genes encoding essential alternative σ factors in BW25113 Δ*relA* Δ*spoT*				
pKT2(*ycbB*) pHV7[c]	IPTG + Ara	31	24	40
pKT2(*ycbB*) pHV17(*rpoH*)	IPTG + Ara	32	26	43
pKT2(*ycbB*) pHV18(*rpoE*)	IPTG + Ara	31	25	41
Overexpression of genes encoding alternative σ factors in BW25113				
pKT2(*ycbB*) pHV17(*rpoH*)	IPTG + Ara	31	18	37
pKT2(*ycbB*) pHV18(*rpoE*)	IPTG + Ara	28	17	33
pKT2(*ycbB*) pHV66(*rpoN*)	IPTG + Ara	30	17	36
pKT2(*ycbB*) pHV67(*rpoS*)	IPTG + Ara	32	19	37
pKT2(*ycbB*) pHV68(*rpoF*)	IPTG + Ara	35	18	40
pKT2(*ycbB*) pHV70(*fecI*)	IPTG + Ara	30	17	37
Overexpression of genes encoding alternative σ factors in BW25113 Δ*ycbB*				
pKT2(*ycbB*) pHV17(*rpoH*)	IPTG + Ara	30	17	32
pKT2(*ycbB*) pHV18(*rpoE*)	IPTG + Ara	29	17	32
pKT2(*ycbB*) pHV66(*rpoN*)	IPTG + Ara	31	17	35
pKT2(*ycbB*) pHV67(*rpoS*)	IPTG + Ara	30	17	36
pKT2(*ycbB*) pHV68(*rpoF*)	IPTG + Ara	33	18	40
pKT2(*ycbB*) pHV70(*fecI*)	IPTG + Ara	29	16	37

[a] The diameter of inhibition zones was determined by the disk diffusion assay using disks containing 10 μg mecillinam (Mel), 10 μg ampicillin (Amp), or 30 μg ceftriaxone (Cro). Data are the medians from three experiments.

[b] The *ycbB* gene carried by plasmid pKT2 was induced with 40 μM IPTG. The *relA'* gene was induced with 1% L-arabinose (Ara). The genes encoding alternative sigma factor were induced with 0.2% L-arabinose.

[c] pHV7 is the vector used for construction of pKT8(*relA'*), pHV17(*rpoH*), pHV18(*rpoE*), pHV66(*rpoN*), pHV67(*rpoS*), pHV68(*rpoF*), and pHV70(*fecI*).

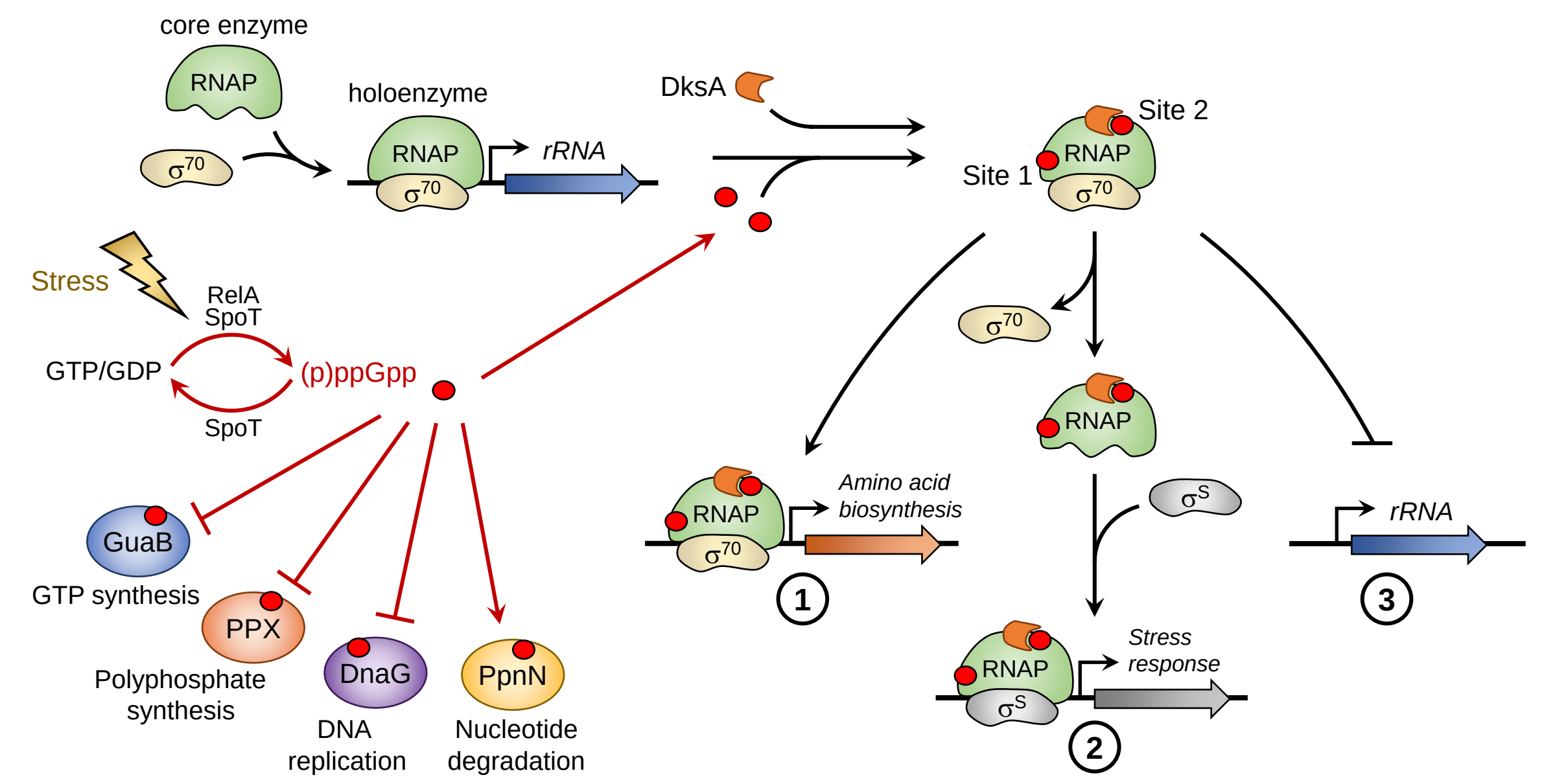
core enzyme
RNAP
σ70
holoenzyme
RNAP
σ70
rRNA
DksA
Site 2
Site 1
RNAP
σ70
Stress
RelA
SpoT
GTP/GDP
(p)ppGpp
SpoT
σ70
RNAP
GuaB
GTP synthesis
PPX
Polyphosphate synthesis
DnaG
DNA replication
PpnN
Nucleotide degradation
RNAP
σ70
Amino acid biosynthesis
1
σS
RNAP
σS
Stress response
2
rRNA
3

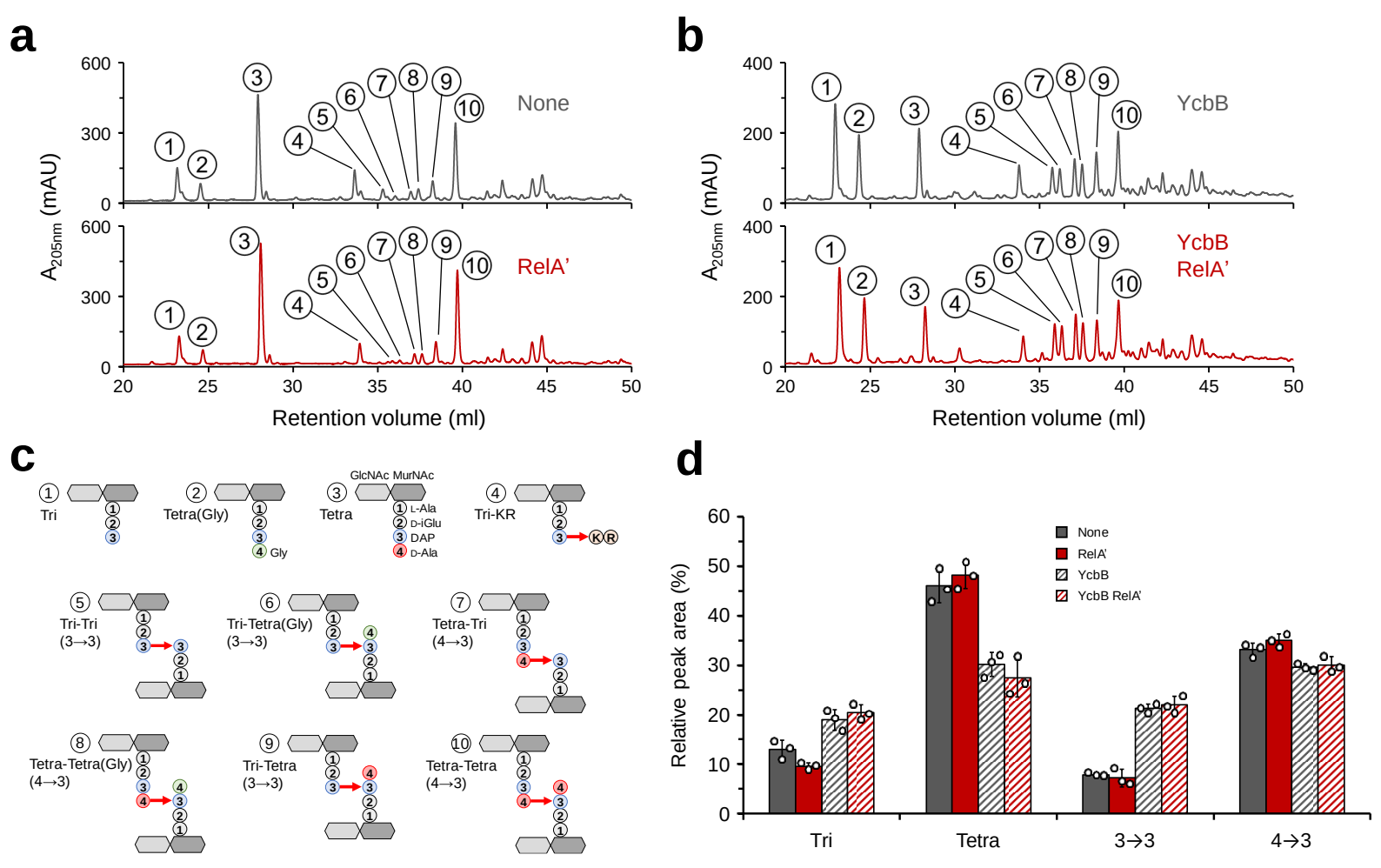
a
b
c
d
None
RelA'
YcbB
YcbB RelA'
A205nm (mAU)
Retention volume (ml)
Tri
Tetra(Gly)
Tetra
Tri-KR
GlcNAc MurNAc
L-Ala
D-iGlu
DAP
D-Ala
Gly
Tri-Tri (3→3)
Tri-Tetra(Gly) (3→3)
Tetra-Tri (4→3)
Tetra-Tetra(Gly) (4→3)
Tri-Tetra (3→3)
Tetra-Tetra (4→3)
Relative peak area (%)
3→3
4→3

a

RNAP substitutions obtained by selection with β-lactams or rifampicin

Substitution (subunit)	Mutation$^{(Selector)}$	GT (min)
Wild-type	None	24 ± 1
β-lactam resistance		
Pro^{153}Leu (β)	CCG→CTG$^{(Mel)}$	ND
Leu^{420}Arg (β)	CTG→CGG$^{(Mel)}$	37 ± 1
Gly^{449}Val (β)	GGC→GTC$^{(Mel)}$	27 ± 1
Gly^{333}Asp (β')	GGT→GAT$^{(Mel)}$	ND
Leu^{1144}Pro (β')	CTC→CCG$^{(Mel)}$	ND
Ala^{1147}Pro (β')	GCA→CCA$^{(Mel)}$	ND
Gly^{1308}Asp (β')	GGT→GAT$^{(Amp)}$	40 ± 2
Rifampicin resistance		
Gln^{148}Leu (β)	CAG→CTG$^{(Rif)}$	28 ± 2
Gln^{148}Arg (β)	CAG→CGG$^{(Rif)}$	28 ± 2
Leu^{149}Arg (β)	CTG→CGG$^{(Rif)}$	28 ± 3
Ile^{572}Leu (β)	ATC→CTC$^{(Rif)}$	28 ± 2
Co-resistance		
His^{447}Leu (β)	CAC→CTC$^{(Amp)}$	48 ± 2
Arg^{451}Cys (β)	CGT→TGT$^{(Amp; Mel)}$	34 ± 2
His^{551}Pro (β)	CAC→CCC$^{(Mel)}$	34 ± 1
Thr^{563}Pro (β)	ACC→CCC$^{(Amp; Mel; Rif)}$	50 ± 3
Gly^{570}Ser (β)	GGT→AGT$^{(Mel)}$	36 ± 3

b

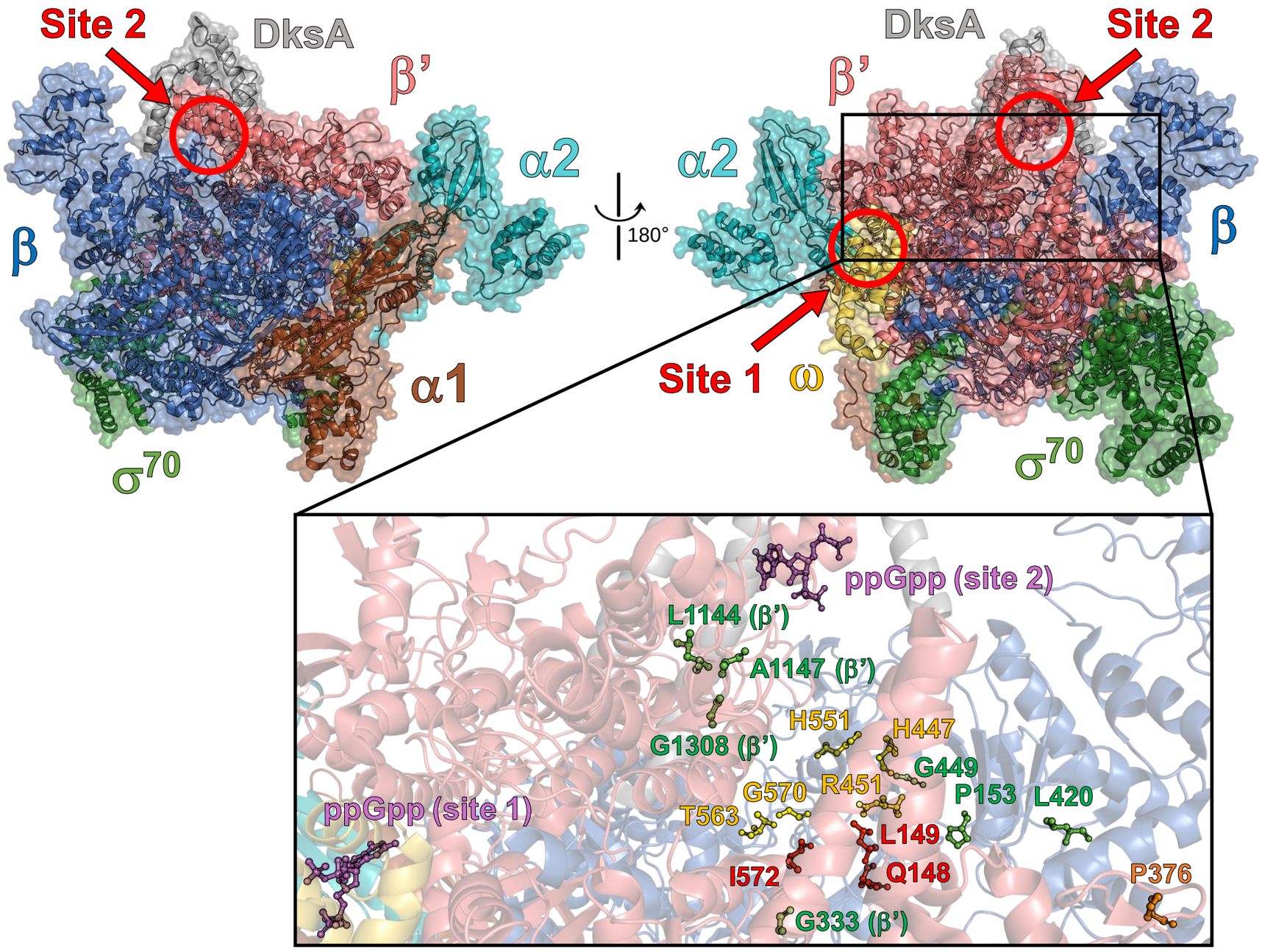

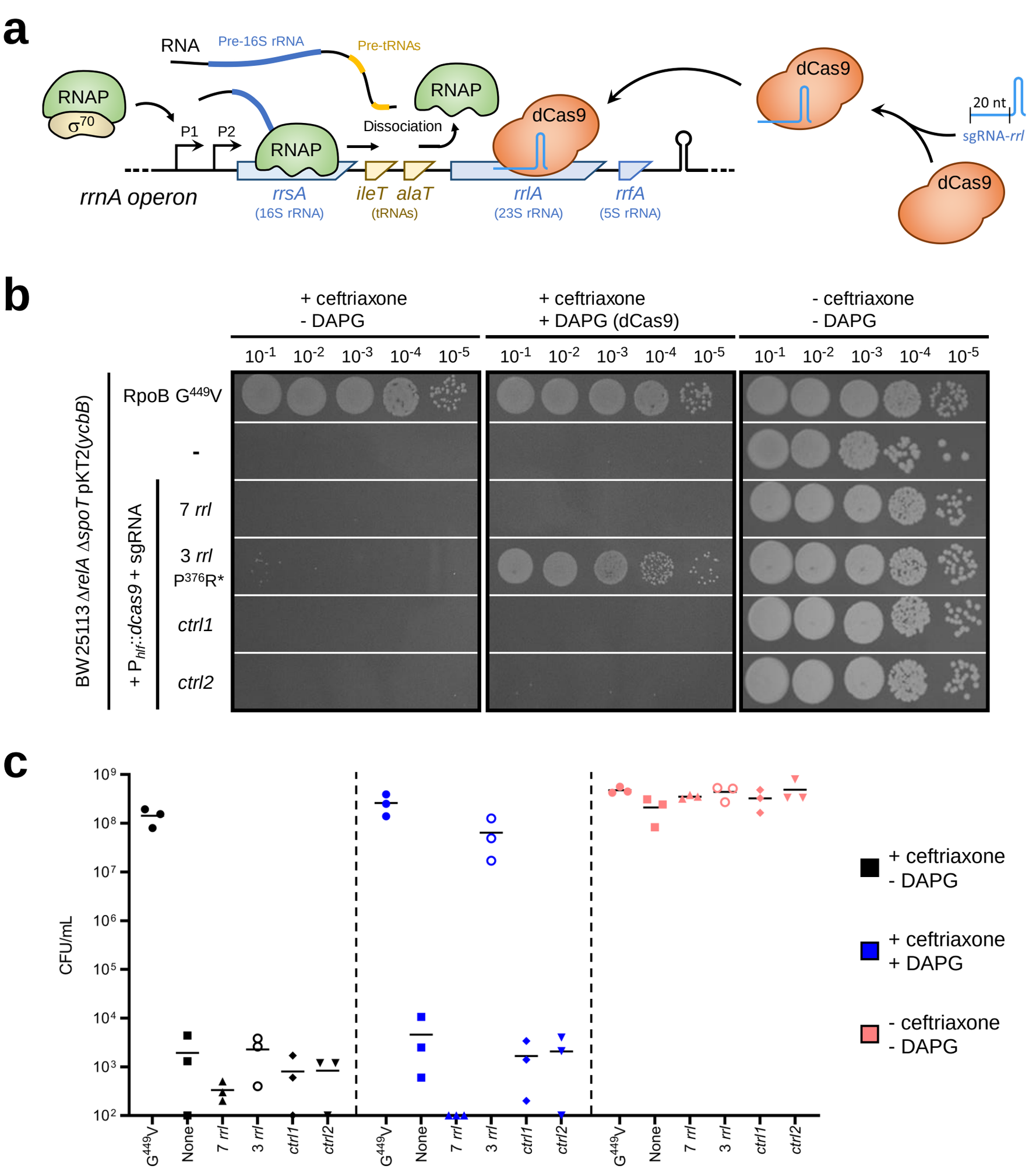
a
RNA
Pre-16S rRNA
Pre-tRNAs
RNAP
σ70
P1
P2
RNAP
Dissociation
RNAP
dCas9
dCas9
20 nt
sgRNA-rrl
dCas9
rrnA operon
rrsA
(16S rRNA)
ileT alaT
(tRNAs)
rrlA
(23S rRNA)
rrfA
(5S rRNA)
b
+ ceftriaxone
- DAPG
+ ceftriaxone
+ DAPG (dCas9)
- ceftriaxone
- DAPG
10-1 10-2 10-3 10-4 10-5
BW25113 ΔrelA ΔspoT pKT2(ycbB)
+ Phif::dcas9 + sgRNA
RpoB G449V
-
7 rrl
3 rrl P376R*
ctrl1
ctrl2
c
CFU/mL
10^9
10^8
10^7
10^6
10^5
10^4
10^3
10^2
G449V
None
7 rrl
3 rrl
ctrl1
ctrl2
+ ceftriaxone
- DAPG
+ ceftriaxone
+ DAPG
- ceftriaxone
- DAPG

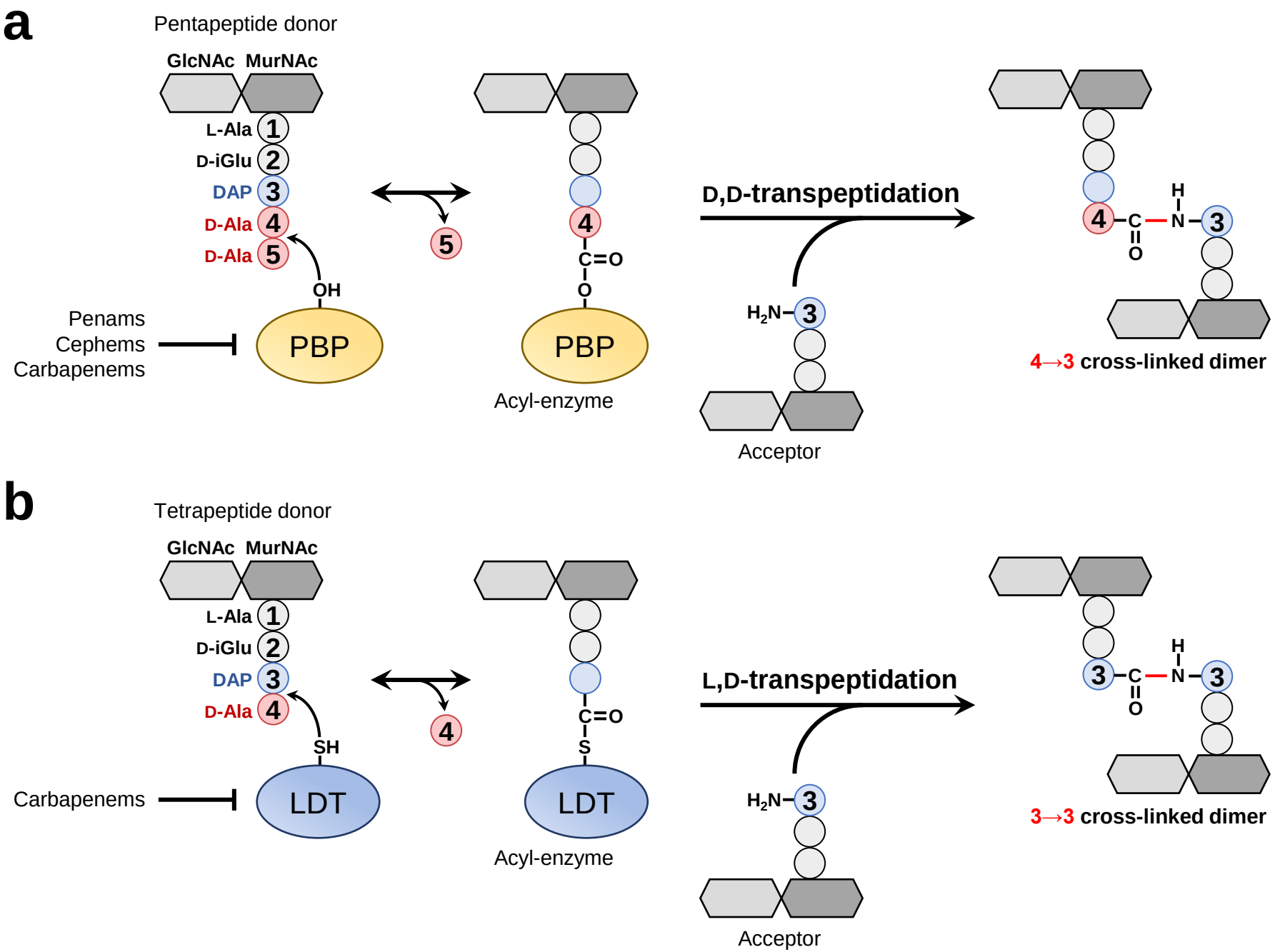
a
Pentapeptide donor
GlcNAc
MurNAc
L-Ala
D-iGlu
DAP
D-Ala
D-Ala
1
2
3
4
5
OH
Penams
Cephems
Carbapenems
PBP
5
C=O
O
PBP
Acyl-enzyme
D,D-transpeptidation
H2N
3
Acceptor
H
N
C
O
4
3
4→3 cross-linked dimer
b
Tetrapeptide donor
GlcNAc
MurNAc
L-Ala
D-iGlu
DAP
D-Ala
1
2
3
4
SH
Carbapenems
LDT
4
C=O
S
LDT
Acyl-enzyme
L,D-transpeptidation
H2N
3
Acceptor
H
N
C
O
3
3
3→3 cross-linked dimer

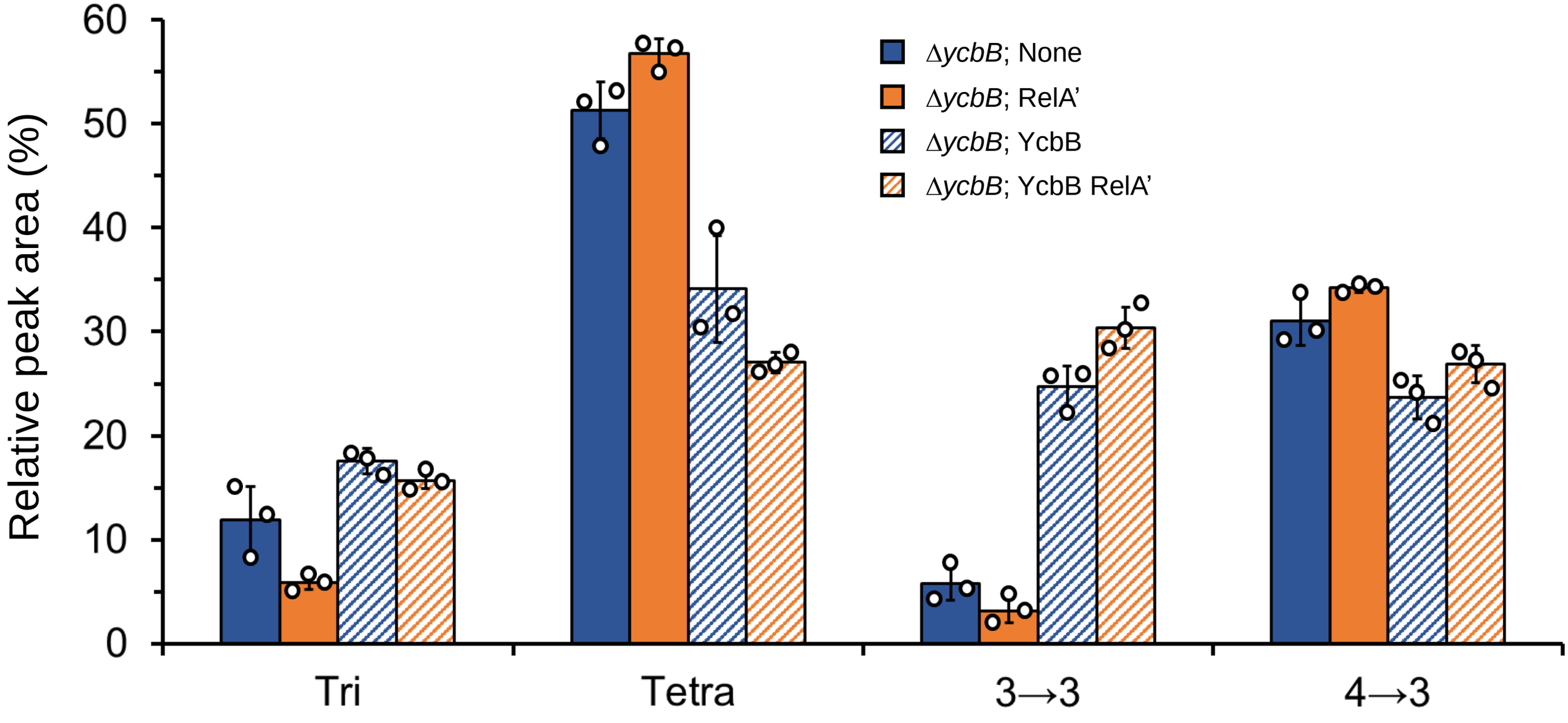
Relative peak area (%)
60
50
40
30
20
10
0
ΔycbB; None
ΔycbB; RelA'
ΔycbB; YcbB
ΔycbB; YcbB RelA'
Tri
Tetra
3→3
4→3

a

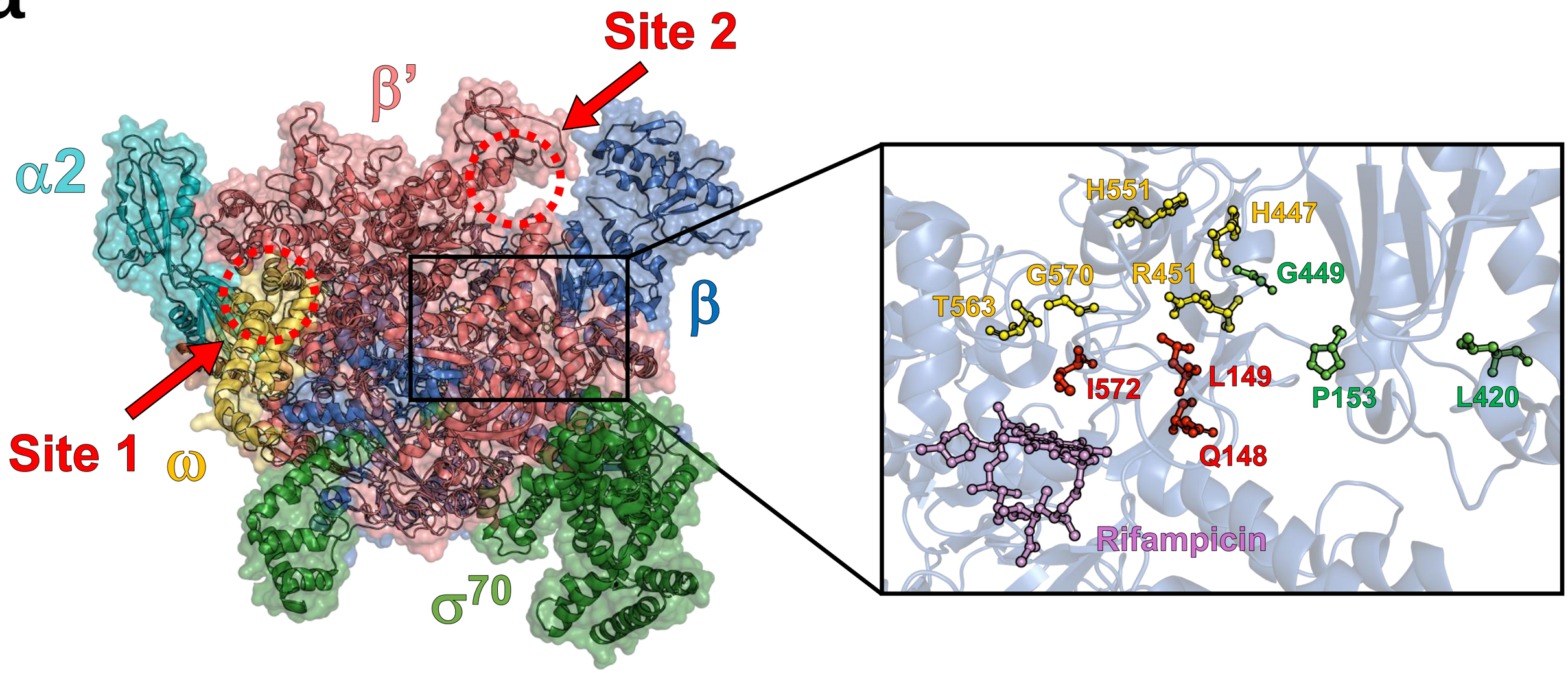
Site 2
β'
α2
β
Site 1
ω
σ70
H551
H447
G570
R451
G449
T563
I572
L149
P153
L420
Q148
Rifampicin

b

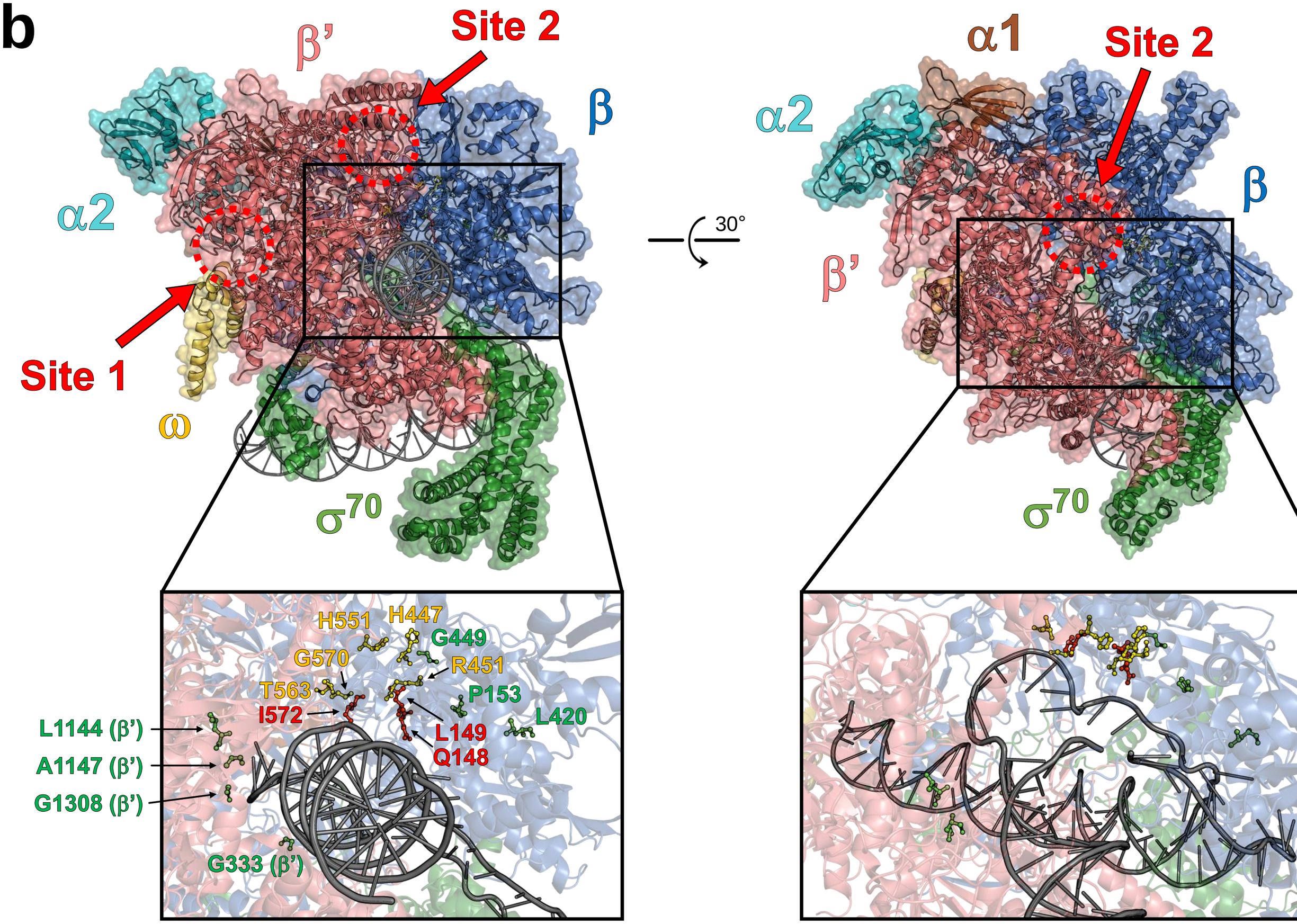
β'
Site 2
β
α2
Site 1
ω
σ70
30°
α1
α2
β
β'
σ70
H551
H447
G449
G570
R451
T563
P153
L420
I572
L149
Q148
L1144 (β')
A1147 (β')
G1308 (β')
G333 (β')

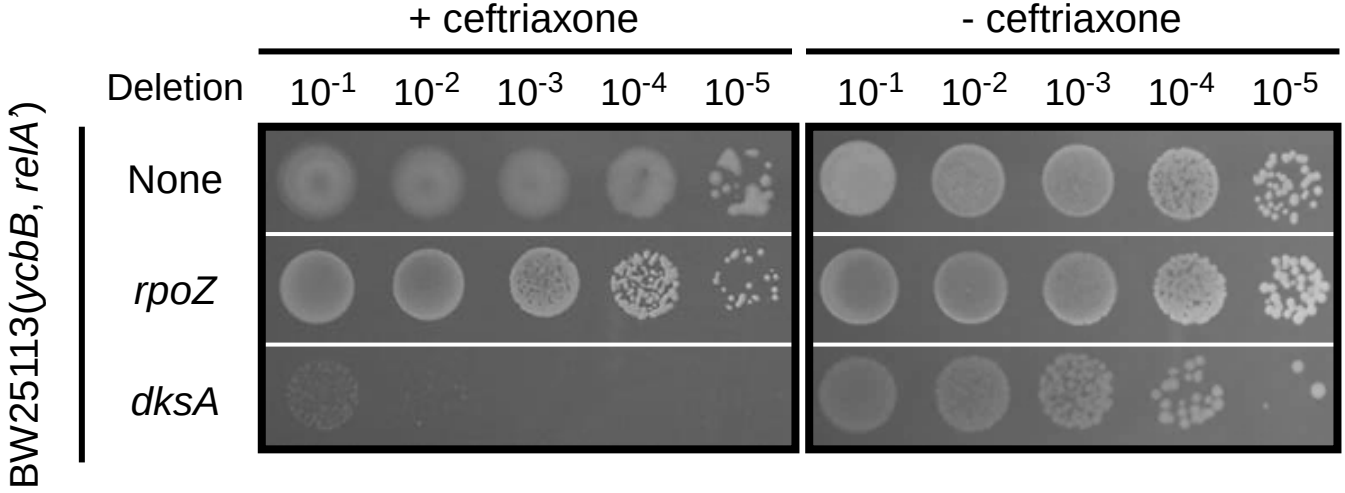
+ ceftriaxone
- ceftriaxone
Deletion
10-1
10-2
10-3
10-4
10-5
10-1
10-2
10-3
10-4
10-5
BW25113(ycbB, relA')
None
rpoZ
dksA

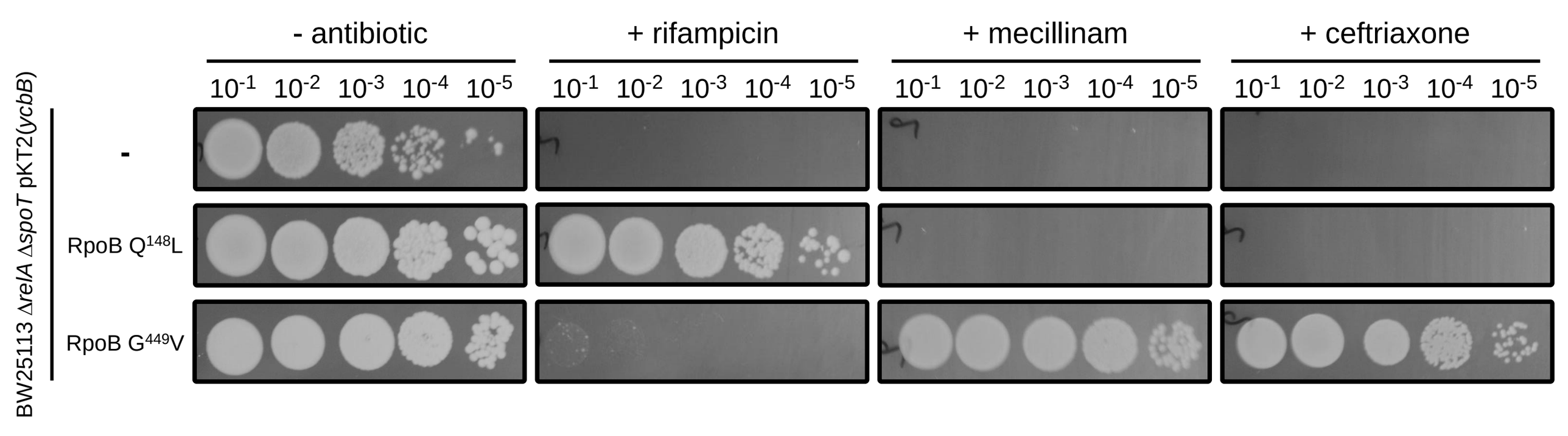
- antibiotic
+ rifampicin
+ mecillinam
+ ceftriaxone
10-1 10-2 10-3 10-4 10-5
BW25113 ΔrelA ΔspoT pKT2(ycbB)
-
RpoB Q148L
RpoB G449V

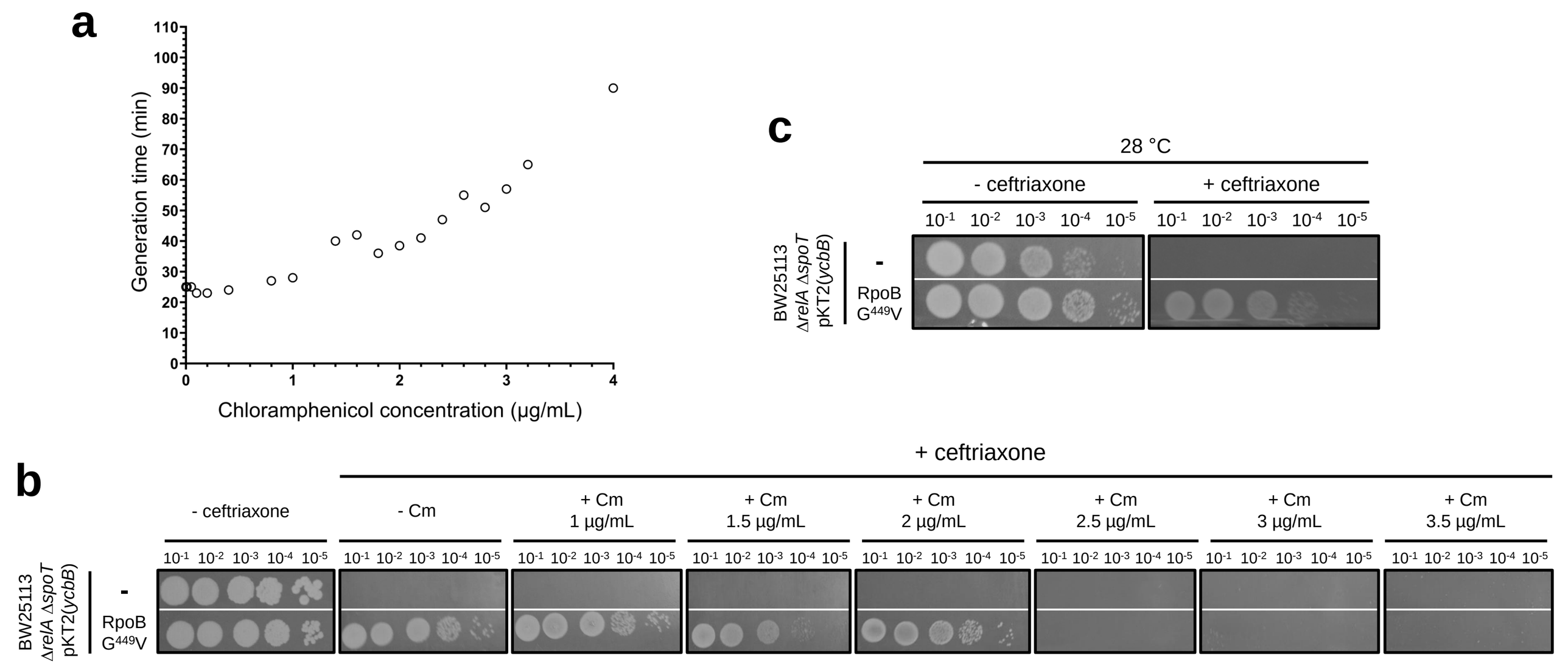
a
Generation time (min)
Chloramphenicol concentration (µg/mL)
c
28 °C
- ceftriaxone
+ ceftriaxone
10-1 10-2 10-3 10-4 10-5
BW25113 ΔrelA ΔspoT pKT2(ycbB)
-
RpoB G449V
b
+ ceftriaxone
- ceftriaxone
- Cm
+ Cm 1 µg/mL
+ Cm 1.5 µg/mL
+ Cm 2 µg/mL
+ Cm 2.5 µg/mL
+ Cm 3 µg/mL
+ Cm 3.5 µg/mL

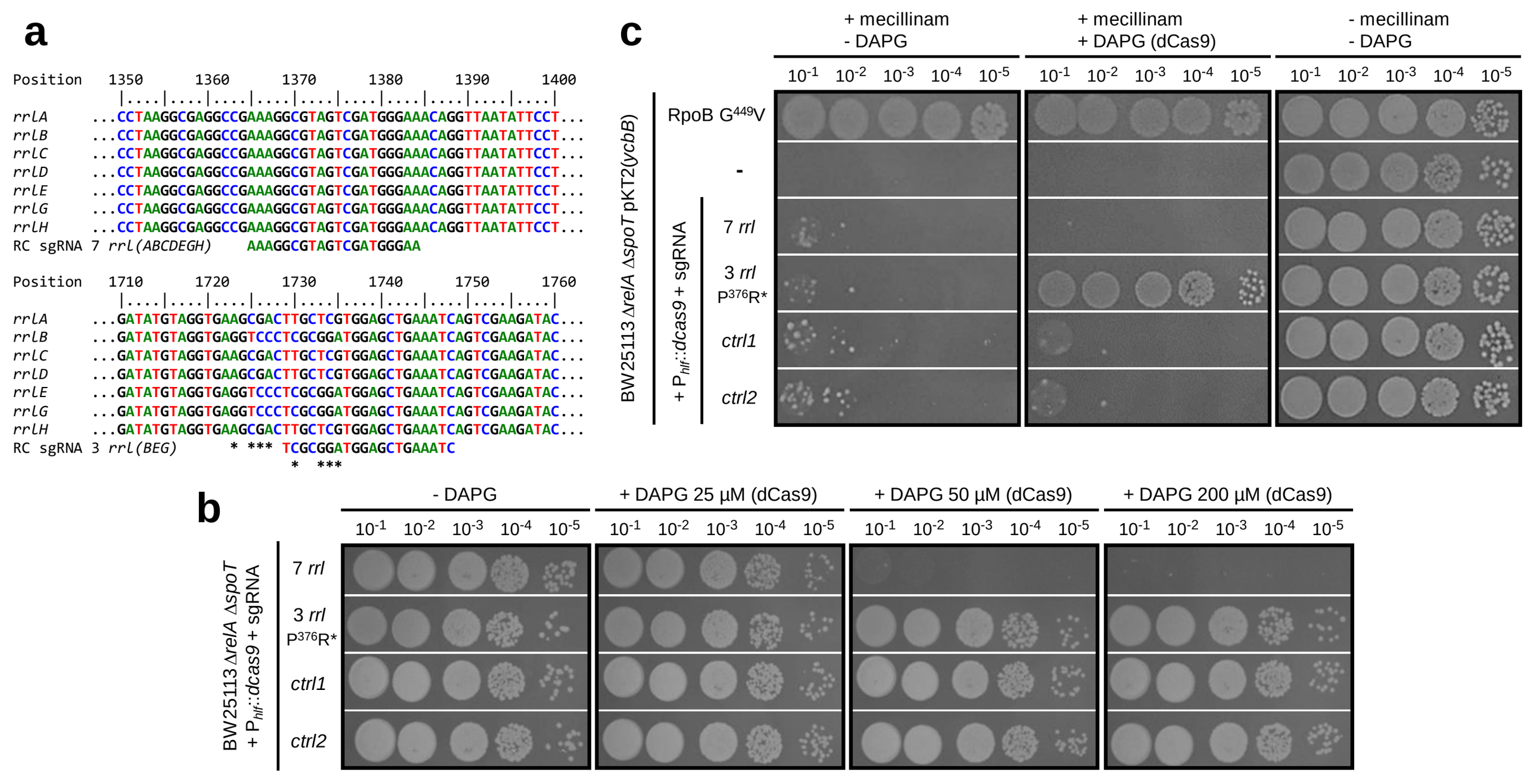
a
Position 1350 1360 1370 1380 1390 1400
rrlA ...CCTAAGGCGAGGCCGAAAGGCGTAGTCGATGGGAAACAGGTTAATATTCCT...
rrlB ...CCTAAGGCGAGGCCGAAAGGCGTAGTCGATGGGAAACAGGTTAATATTCCT...
rrlC ...CCTAAGGCGAGGCCGAAAGGCGTAGTCGATGGGAAACAGGTTAATATTCCT...
rrlD ...CCTAAGGCGAGGCCGAAAGGCGTAGTCGATGGGAAACAGGTTAATATTCCT...
rrlE ...CCTAAGGCGAGGCCGAAAGGCGTAGTCGATGGGAAACAGGTTAATATTCCT...
rrlG ...CCTAAGGCGAGGCCGAAAGGCGTAGTCGATGGGAAACAGGTTAATATTCCT...
rrlH ...CCTAAGGCGAGGCCGAAAGGCGTAGTCGATGGGAAACAGGTTAATATTCCT...
RC sgRNA 7 rrl(ABCDEGH) AAAGGCGTAGTCGATGGGAA
Position 1710 1720 1730 1740 1750 1760
rrlA ...GATATGTAGGTGAAGCGACTTGCTCGTGGAGCTGAAATCAGTCGAAGATAC...
rrlB ...GATATGTAGGTGAGGTCCCTCGCGGATGGAGCTGAAATCAGTCGAAGATAC...
rrlC ...GATATGTAGGTGAAGCGACTTGCTCGTGGAGCTGAAATCAGTCGAAGATAC...
rrlD ...GATATGTAGGTGAAGCGACTTGCTCGTGGAGCTGAAATCAGTCGAAGATAC...
rrlE ...GATATGTAGGTGAGGTCCCTCGCGGATGGAGCTGAAATCAGTCGAAGATAC...
rrlG ...GATATGTAGGTGAGGTCCCTCGCGGATGGAGCTGAAATCAGTCGAAGATAC...
rrlH ...GATATGTAGGTGAAGCGACTTGCTCGTGGAGCTGAAATCAGTCGAAGATAC...
RC sgRNA 3 rrl(BEG) * *** TCGCGGATGGAGCTGAAATC
* ***
c
+ mecillinam
- DAPG
+ mecillinam
+ DAPG (dCas9)
- mecillinam
- DAPG
10-1 10-2 10-3 10-4 10-5
BW25113 ΔrelA ΔspoT pKT2(ycbB)
+ Phif::dcas9 + sgRNA
RpoB G449V
-
7 rrl
3 rrl P376R*
ctrl1
ctrl2
b
- DAPG
+ DAPG 25 µM (dCas9)
+ DAPG 50 µM (dCas9)
+ DAPG 200 µM (dCas9)
10-1 10-2 10-3 10-4 10-5
BW25113 ΔrelA ΔspoT
+ Phif::dcas9 + sgRNA
7 rrl
3 rrl P376R*
ctrl1
ctrl2

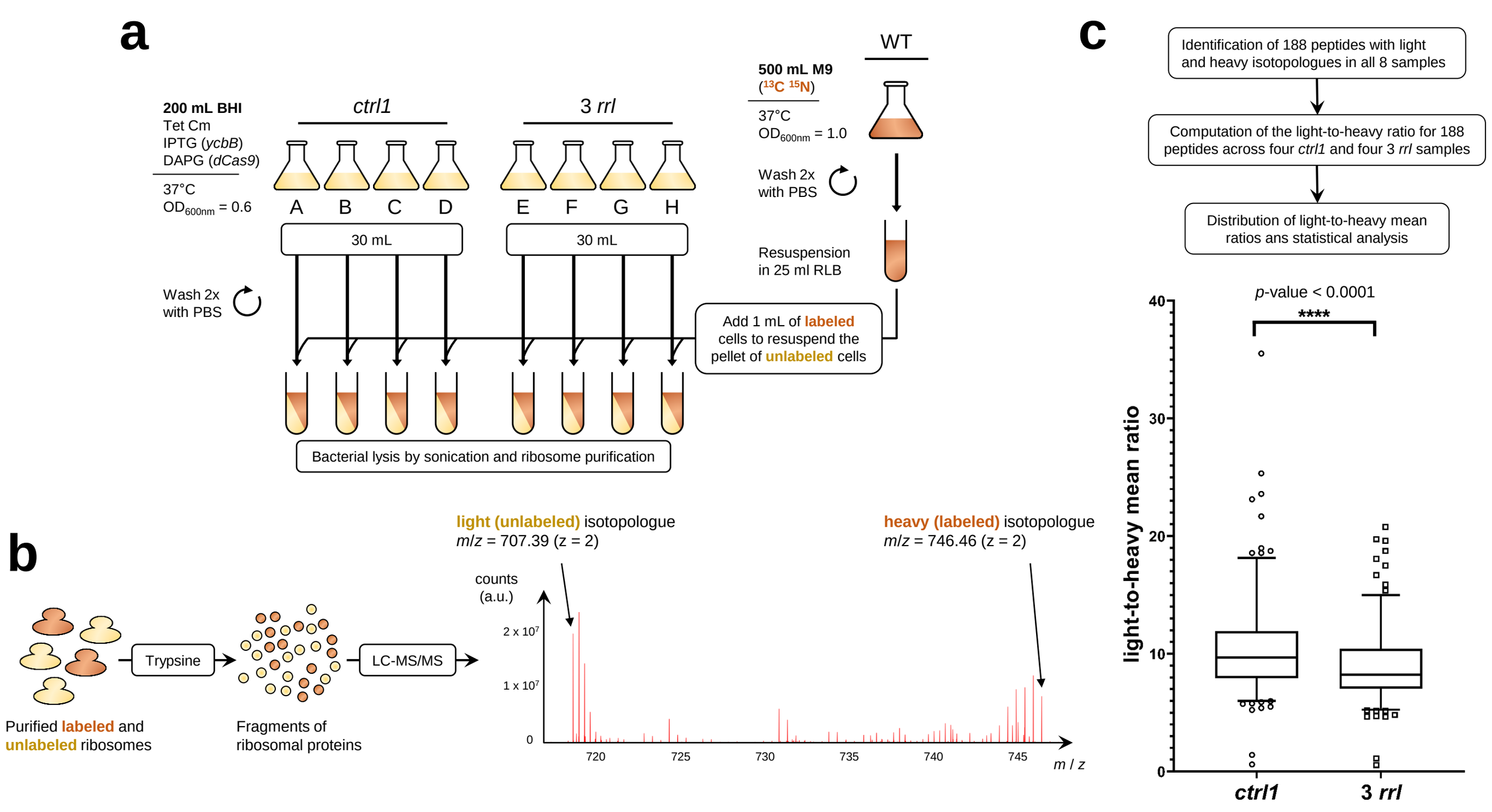
a
200 mL BHI
Tet Cm
IPTG (ycbB)
DAPG (dCas9)
37°C
OD600nm = 0.6
ctrl1
3 rrl
A B C D
E F G H
30 mL
30 mL
Wash 2x with PBS
WT
500 mL M9
(13C 15N)
37°C
OD600nm = 1.0
Wash 2x with PBS
Resuspension in 25 ml RLB
Add 1 mL of labeled cells to resuspend the pellet of unlabeled cells
Bacterial lysis by sonication and ribosome purification
b
Trypsine
LC-MS/MS
Purified labeled and unlabeled ribosomes
Fragments of ribosomal proteins
light (unlabeled) isotopologue
m/z = 707.39 (z = 2)
heavy (labeled) isotopologue
m/z = 746.46 (z = 2)
counts (a.u.)
2 x 10^7
1 x 10^7
0
720
725
730
735
740
745
m / z
c
Identification of 188 peptides with light and heavy isotopologues in all 8 samples
Computation of the light-to-heavy ratio for 188 peptides across four ctrl1 and four 3 rrl samples
Distribution of light-to-heavy mean ratios ans statistical analysis
p-value < 0.0001
****
light-to-heavy mean ratio
40
30
20
10
0
ctrl1
3 rrl

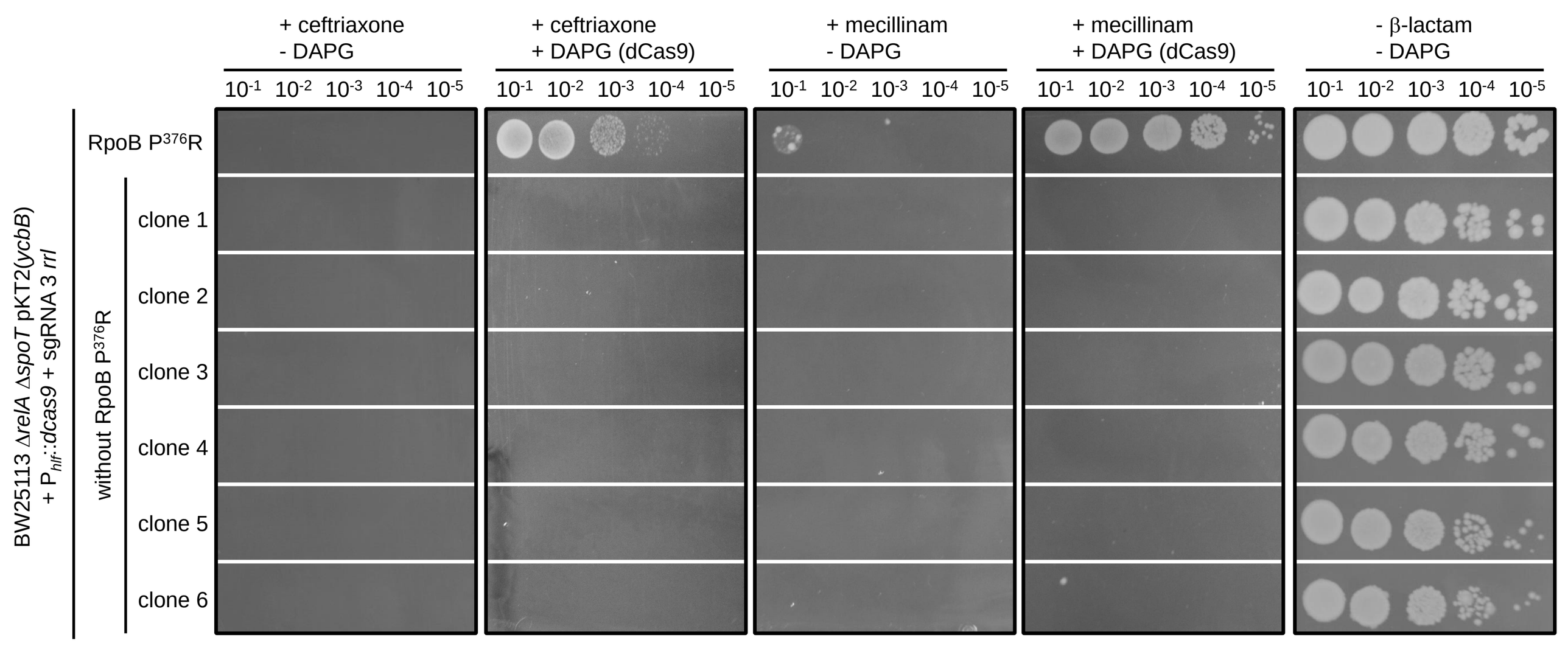
+ ceftriaxone
- DAPG
+ ceftriaxone
+ DAPG (dCas9)
+ mecillinam
- DAPG
+ mecillinam
+ DAPG (dCas9)
- β-lactam
- DAPG
10-1 10-2 10-3 10-4 10-5
BW25113 ΔrelA ΔspoT pKT2(ycbB)
+ Phlf::dcas9 + sgRNA 3 rrl
RpoB P376R
without RpoB P376R
clone 1
clone 2
clone 3
clone 4
clone 5
clone 6